UNIVERSIDADE DA BEIRA INTERIOR
Engenharia

Effects of Design Parameters on Damping of Composite Materials for Aeronautical Applications

João Pedro dos Santos Lopes

Dissertation for the Degree of Master of Science in

Aeronautical Engineering

Supervisor: José Miguel Almeida da Silva, PhD
Co-supervisor: Pedro Vieira Gamboa, PhD

Covilhã, June 2013

Acknowledgments

I would like to express my sincere gratitude to my parents, who were tireless during all these University years providing me the possibility to study far away from home and in a course which I really love.

A very special kind of gratitude to Professor José Miguel Silva, my academic supervisor, for his support and guidance both in my thesis and in the parallel scientific works. Moreover, for his classes in aerospace structures and materials, which have inspired me to develop this thesis in the area of composite polymers and vibration control.

To Professor Pedro V. Gamboa, my co-supervisor, for his assistance and suggestions, and also, not less important, for all the provided laboratory conditions and material.

To Professors Ricardo Claudio and Nuno Nunes, from Instituto Politécnico de Setúbal, for their attention, time and support during the experimental works, as well as their receptiveness during the time I spent in IPS.

And a sincere acknowledgement to Filipe Couceiro (PhD student) and Alejandro Píriz (former MSc student) for their help during my thesis work. I hope to return their support one day!

Dedicated to my Professors, to my Parents and Family and to my unforgettable University friends!

Abstract

Many engineering projects have shown a great concern with the dynamic response of generalized mechanical systems where a set of rigorous demands are placed on the design of structures in sectors such as the aerospace or the automobile industries. Aerospace materials, for example, in most cases have been developed for a specific purpose, like some particular metal alloys and composites. It is their operation requirements that influence the optimization of certain intrinsic mechanical or physical properties.

The dynamic behaviour of a structure can be refined by anticipating any performance-related problem during the design process, where vibration and others parameters can be measured and optimized for the desired applications. It is often desirable to be able to predict accurately the dynamic response of a structure under certain excitation conditions. Given that, it is necessary to understand how its mass, stiffness or damping properties could be modified to obtain a desired response and vibration control, taking into account structural margin of safety and life-time limits under service. Thus, the damping of such structures, which is associated to the energy dissipation capacity, is a key aspect regarding the fatigue endurance and noise/vibration control as it controls the amplitude of resonant vibration response.

Envisaging to create a cheaper, direct and maintenance-free alternative to active damping systems, passive methods are a straightforward solution for certain industrial demands. In fact, active damping systems typically imply more structure weight, considerable energy consumption, reliability issues and limited strain/force response, which are undesired features in general technological applications, especially in the aerospace sector. To achieve high damping properties discarding the use of an active system, the use of some isolation techniques, the inclusion of high damping materials or even the need for physical structural modifications are often necessary in the standpoint of a new component's development for passive control applications. As an example, in most recent investigations, co-curing/embedded viscoelastic damping constituents in composites has been a successful way to increase the damping capacity.

In the context of the present work, a passive damping treatment method based on cork utilization as viscoelastic material has been used to improve the damping properties of fiber-reinforced composites. A numerical and experimental study was made to predict and understand the benefits of such method and characterize any inherent effects on modal loss factor and respective structural natural frequencies regarding the use of cork. The excellent energy absorption properties of cork under static and dynamic loading conditions, its lightness, near-impermeability and lower thermal conductivity, are the base of a recent and

crescent interest in aeronautical, railroad and automobile applications for cork based materials. These intrinsic characteristics are also the main reasons for considering it as viscoelastic layer applicable in passive damping treatments with a great potential for vibration control in future aerospace applications.

As far as the numerical study concerns, a finite element model (FEM) was developed to analyze the main dynamic properties of the composite structure samples, for example, the modal frequencies and respective loss factors, and compare it with the experimental results, allowing to assess the accuracy of numerical data. Distinct design variables were considered to determine their influence in the loss factor variation, namely: damping layer thickness and its relative position within the laminate, number of viscoelastic layers and effect of different layup stacking sequences.

Results are encouraging about the possible use of cork based composites as a viable passive solution to improve the damping properties of high performance composites, giving rise to an increase of the loss factor as well as a change of the natural frequencies of the structure according to the design requirements for particular applications.

Keywords

Damping, composites materials, viscoelastic materials, loss factor, cork.

Resumo

A resposta dinâmica de sistemas mecânicos revelou ser de grande preocupação em vários projectos de engenharia onde existe um conjunto rigoroso de exigências ligadas ao projecto de estruturas, tal como acontece em particular na indústria aeroespacial e automóvel. Materiais aeroespaciais, por exemplo, foram em muitos dos casos desenvolvidos tendo em conta propósitos específicos, tais como algumas ligas metálicas e alguns compósitos. São os requisitos de operação que influenciaram a optimização de certas propriedades mecânicas ou físicas desses materiais.

O comportamento dinâmico de uma estrutura pode ser refinado durante o processo de projecto antecipando qualquer problema relacionado com o respectivo desempenho, onde vibrações e outros parâmetros podem ser medidos e posteriormente optimizados tendo em conta as aplicações desejadas. É preferível ter capacidade para prever com precisão a resposta dinâmica de uma estrutura exposta a determinadas condições de vibração. Posto isto, é necessário entender como é que a respectiva massa, rigidez ou as propriedades de amortecimento podem ser modificadas de forma a obter um controlo desejado de comportamento e vibração, tendo em conta as margens de segurança e limites de vida útil estruturais durante a sua operação. Assim, o amortecimento de tais estruturas, que está associado com a capacidade de dissipação de energia, é um aspecto chave relativamente à resistência à fadiga e no controlo de ruido/vibração traduzindo-se na forma como é controlada a amplitude de resposta em vibrações de ressonância.

Pretendendo criar uma alternativa ao controlo de vibrações activo mais barata e com pouca necessidade de manutenção, os métodos passivos apresentam-se como uma solução directa a algumas necessidades da indústria. De facto, a aplicação de sistemas activos tipicamente implica mais peso estrutural, um considerável consumo de energia, problemas de reabilitação e uma resposta deformação/tensão limitada, as quais são características indesejadas para as aplicações tecnológicas gerais, especialmente para o sector aeroespacial. Para conseguir melhores propriedades de amortecimento descartando o uso de um sistema activo, o uso de algumas técnicas de isolamento, a inclusão de materiais de alto amortecimento e até a necessidade de modificações físicas e estruturais são frequentemente necessárias no ponto de vista de o desenvolvimento de um novo componente para aplicações de controlo passivo. Como exemplo, investigações recentes apresentam certos compósitos pós-curados com camadas viscoelásticas embebidas como uma forma bem sucedida de aumentar as capacidades de amortecimento.

No contexto do trabalho presente, um método de tratamento de amortecimento passivo baseado na utilização da cortiça como um material viscoelástico foi utilizado para melhorar

as propriedades de amortecimento de compósitos com fibras de reforço. Foi então elaborado um estudo numérico e experimental para prever e entender os benefícios de tal método caracterizando qualquer efeito inerente no factor de perda e nas respectivas frequências naturais estruturais. As excelentes propriedades de absorção de energia por parte da cortiça sobre condições de carregamentos estáticos e dinâmicos, a sua baixa densidade volumétrica, quase impermeabilidade e baixa condutividade térmica, são a base de um recente e crescente interesse da sua aplicação precisamente no sector aeronáutico, ferroviário e automóvel.

Em relação ao estudo numérico, um modelo de elementos fintos (MEF) foi desenvolvido em software ABAQUS® para analisar as principais propriedades dinâmicas de provetes feitos em compósito, como por exemplo as frequências modais e respectivo factor de perda, comparando-as posteriormente com os resultados experimentais permitindo então classificar a precisão dos dados numéricos. Distintas variáveis de projecto foram consideradas para determinar a sua influência na variação do factor de perda, nomeadamente: a espessura da camada viscoelástica e a sua posição relativa no laminado, o número de camadas viscoelásticas e o efeito das diferentes sequências de empilhamento.

Os resultados são optimistas em relação à possibilidade do uso da cortiça em compósitos como um método passivo viável tendo em conta o aumento do factor de perda bem como na modificação das frequências naturais da estrutura de acordo com os requisitos de projecto de cada aplicação.

Palavras-chave

Amortecimento, materiais compósitos, materiais viscoelásticos, factor de perda, cortiça.

Contents

List of Figures

List of Tables

Nomenclature

α	Mass proportional damping factor
β	Stiffness proportional damping factor
$[\mathrm{C}]$	Damping matrix of the system
$[\mathrm{M}]$	Mass matrix of the system
$[\mathrm{K}]$	Stiffness matrix of the system
X	Position vector
$\dot{X}$	Velocity vector
$\ddot{X}$	Acceleration vector
$[\mathrm{F(t)}]$	External load vector
$\{U\}$	Harmonic response
$\emptyset$	Eigenvector for each vibration mode
G_R	Shear relaxation modulus
g_R	Dimensionless shear relaxation modulus
G_0	Instantaneous shear modulus
G_∞	Long-term shear modulus
G	Shear modulus
G^*	Complex shear modulus
G’	Storage shear modulus
G’’	Loss shear modulus
E^*	Complex Young’s modulus
E’	Storage Young’s modulus
E’’	Loss Young’s modulus
K	Bulk modulus
K_0	Instantaneous bulk modulus
K_∞	Long-term bulk modulus
K^*	Complex bulk modulus
K’	Storage bulk modulus
K’’	Loss bulk modulus
υ	Poisson’s ratio
υ^*	Complex Poisson’s ratio
υ'	Poisson’s dynamic ratio
υ''	Poisson’s loss ratio
C_n	Corrector factor
EI	Flexure rigidity
σ	Stress
ε	strain

μ	Viscosity of the material
τ	Reduced time
$\overline{g_i^P}$	Shear modulus Prony series terms
$\overline{k_i^P}$	Bulk modulus Prony series terms
i	Complex number ($\sqrt{-1}$)
ω	Frequency
t	Time
θ	Temperature
η	Loss factor
ξ	Damping ratio
ψ	Specific damping capacity
CFRP	Carbon fiber reinforced polymer
FEM	Finite element method
RKU	Ross–Kerwin-Ungar damping model
C	NL 10 $Corecork^{®}$ agglomerate (Cork layer)

Chapter 1

Introduction

1.1 Motivations for studying damping in composites and viscoelastic materials

The worldwide aeronautical industry, as many other industrial sectors, is experiencing a restructuring process in order to achieve the efficiency and productivity levels required to meet the challenges of the market demands in the first quarter of the twenty-first century. In the late 60's, carbon fiber became a serious material for lightweight applications. The specific strength and rigidity modulus of high strength fiber composites are higher than other comparable metallic alloys. For the aeronautic industry it means greater weight savings resulting in improved aircraft's performance, greater payloads, longer range and fuel savings. The first large scale usage of composites in commercial aircraft occurred in 1985, when the Airbus A320 introduced composite horizontal and vertical stabilizers. Airbus has also applied composites in up to 15% of the overall airframe weight for their A320, A330 and A340 family [1, 2]. More recently, the new Boeing 787 is a revolutionary commercial airliner made mostly of carbon composites or super durable plastic representing over than 50 % of the empty weight. However, the use of composites has been more prominent in the military sector, spreading surprisingly to general aviation aircraft in the following decades.

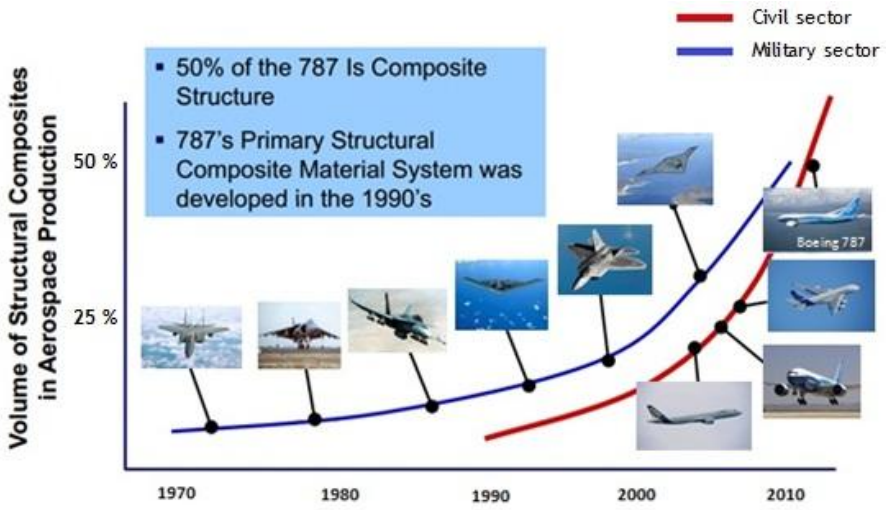

Figure 1 – Volume of structural composites application in military and civil aerospace production over the last decades.

The increased use of composites in aerospace, automobile and railroad sectors revealed a new state of problems regarding their application compatibility with others materials, particularly for vibro-acoustic control. For general aircraft or some spacecraft, vibrations may have several causes: extension and retraction of landing gear systems, deployment of aerodynamic brakes, engine normal operation and normal airflow over the surfaces. Most of these effects are mainly predominant during the take-off and landing phases. Notwithstanding their inevitability, these vibrations must be minimized by appropriate design features through active and/or passive damping treatments in order to improve aircraft performance and reliability levels of structures and systems.

Passive damping treatments in composites as a result of the application of embedded viscoelastic materials (which possess an intrinsic capacity of dissipating mechanical energy) revels to have greater advantages in terms of energy efficiency and reliability of machines/structures compared to active systems. Presently, there are a considerable number of research works concerning noise and vibration control related to aircraft. For example, by improving interior sound quality, aircraft engineers can increase the passengers comfort. Additionally, other problems regarding air traffic increase in urban areas can be minimized by reducing the engines' exterior noise. For such concerns, materials with damping capabilities used for structural applications, such as the ones with viscoelastic properties, may present a dynamic behaviour that needs a profound knowledge aiming at a better understanding of the their performance under different loading conditions.

In the particular case of passive damping applications in composites via the inclusion of viscoelastic material, studies have been made regarding their use as noise control treatment to reduce noise transmission through automobiles, trains and aircraft fuselage skin panels. This type of damping is also used to decrease the vibro-acoustic response of avionics equipment in typical satellite systems and to maximize the damping capacity of composites used in deployable space structures, such as solar sails, inflatable antennas, inflatable solar arrays, etc. [3, 4].

In the case of this work, a cork agglomerate layer was considered for damping purposes. The reason for considering cork as the viscoelastic material comes from the excellent energy absorption properties of this natural material, which were confirmed in previous works regarding the characterization of cork based composites under static and dynamic loading conditions [5-7]. For engineering purposes, an analysis or design involving cork agglomerates with CFRP must incorporate their viscoelastic behaviour, temperature and frequency dependence as well as the dynamic response, which in general is based on experimental and numerical measurements.

1.2 Objectives

The present thesis characterizes the application of a constrained viscoelastic layer in CFRP specimens as a passive damping treatment. Such damping solution may be applied into structures or mechanical systems that are subjected to loads or cycle excitations which may endanger its strength or cause displacements beyond the design point. The damping of such structures is also important in aspects regarding fatigue endurance, noise and vibration control.

In order to predict the best solution for operational purposes, various laminates with different stacking sequences, number of carbon-fiber layers and viscoelastic layer thickness were characterized via FEM analysis (Finite element method) corroborated with experimental results. As referred before, the viscoelastic material was composed by a cork agglomerate, being necessary to model such material in ABAQUS® 6.10-1 software for a numerical analysis. The FEM analysis was developed in the same software to obtain the main dynamic properties of the structure, such as the natural frequencies and loss factor, as this latter parameter is commonly used as an effective damping evaluator. Experimental testing provided loss factor results for comparison purposes with the numerical data. Results provide useful information about the possible use of cork based composites as a viable passive solution to improve the damping properties of high performance composites, allowing the loss factor evaluation for different laminate's configuration types.

1.3 Thesis structure

This thesis is structured in five chapters. The present one is an introduction to the core theme of this work and respective objectives are presented.

The second chapter summarizes all the essential thesis bibliographic review based on the state-of-the-art performed in the research phase of the work. The main subjects addressed are composite vibration control methods, general theory of structural vibration, composite sandwich structures, structural damping models, viscoelastic models and some information about the half-power bandwidth method used to estimate the experimental loss factor results.

The numerical model developed in this work is described in the third chapter. There is a description of some fundamental concepts regarding the development of the numerical model based on the finite element method (FEM). The main configurations and geometric dimensions of the plate samples are also described in this chapter, as well as the numerical model mesh

convergence study and the necessary model validation through the comparison between numerical end experimental results.

The fourth chapter presents all numerical results obtained in the course of this work followed by a final parametric optimization of the loss factor based in the design parameters effects on damping. The natural frequencies regarding the first bending modes of each beam were also determined through a modal analysis. Moreover, FEM analysis provides important information about the natural mode shapes and frequencies of the different CFRP laminates. Therefore, the requested numerical output is always analysed in a comparative basis on the dynamic behaviour between specimens with or without viscoelastic layer.

Finally, chapter 5 summarizes the major conclusions and suggests possible paths for further developments in the context of this research line.

Chapter 2

Bibliographical review

2.1 Vibration control in composites

Vibrations can be defined as mechanical oscillations of a system which is displaced from its position of equilibrium. Every object has a different response to excitations depending on material properties, geometry, and boundary conditions. For any material, it is convenient to describe the vibrational response by considering three main parameters: amplitude, vibration mode shape and frequency.

Active and passive damping methods provide fundamental capability to control displacements in dynamic load conditions and to prevent undesired vibrations. Nowadays, transport industries (such as aeronautics, railroad and automobile) use many forms of these two methods for vibration and noise suppression purposes, staring the future in a continuous searching for new solutions regarding important design parameters, like structural weight, material and damping systems costs and others aspects dependent on the type of application. The use of composites increased during the last decade due to some important properties, namely their high strength-to-weight ratios (as a result of the superior strength and stiffness of the reinforcing fibers), great corrosion resistance, improved fatigue life and greater design flexibility for optimum mechanical performance. However, the high stiffness of such materials entails a low damping loss factor, which is a measure of energy dissipation capacity. To achieve high damping properties without the use of an active system (which typically implies more structural weight, considerable energy consumption and limited strain/force response) it is necessary to adopt passive approaches, e.g., physical structural modifications, isolation techniques or the use of high damping materials.

From recent investigations, co-curing/embedded viscoelastic damping materials in composites has been a successful way to increase the damping capacity of composites, compromising however the stiffness and strength of the structure (generally affected with little reductions) [8]. The principle is similar to the conventional constrained layer treatment, where the most part of the damping effect comes from the shear loading induced between the damping layer and the constraining layers. Early studies have concluded that the lay-up sequence and the mode of vibration affect the system loss factor, which have significant dependence when combined with others parameters [9-11]. It is the layer deformation in shear mode that leads to energy dissipation in a more efficient way. In addition, sandwich beams with a viscoelastic core are very effective in reducing and controlling vibration response of lightweight and

flexible structures, because in these cases the viscoelastic material is strongly deformed in shear due to the adjacent stiff layers [2]. In flexural vibrations, for a general case of constrained viscoelastic core layer, the dissipation of energy happens due to shear strain in the core, reducing the overall structure vibration. In the unconstrained layers, like the adjacent layers bonded to the core, the dissipation of energy is by means of extension and compression of viscoelastic layer [3, 13].

Attempting to model such behaviour, the utilization of advanced optimization procedures based in the development of computational models reveals to be an efficient procedure to determine structural damping parameters, such as loss factor or damping ratio. For composites with a constrained viscoelastic layer applied through a co-curing process, the anisotropy of fiber-reinforced constrained layers promotes the damping mechanisms due to the higher capacity of energy dissipation of composites when compared with metallic layers, which are an example of conventional isotropic materials [5, 12]. In general, composite materials, especially carbon fiber reinforced polymers (CFRP), have not a high damping capacity and need some improvements using vibration control methods to optimize the damping properties without neglecting the overall component/system weight. The damping of composites depends on the contribution of several micromechanical, laminate and structural parameters, fiber and matrix ratios, ply angles, ply thicknesses, stacking sequence, curing process, temperature and existing damage or structural defects. Moreover, composite damping is anisotropic, where the maximum energy dissipation is verified in the transverse direction and in shear motion whereas the minimum occurs in the direction of the fibers [13]. Aiming at obtaining significant structural advantages of damping in composite materials, it is very important to use adequate analysis tools, where the variables are the parameters of the laminate for damping optimization purposes. Passive damping has been demonstrated as an essential dynamic and viable method for composite vibration suppression as well as in noise control, fatigue endurance and impact resistance [14, 15], which motivated the adoption of this strategy in the present work.

2.1.1 Active control vs passive control

Active control

Active control is applied, in general, with attached mechanisms and devices, needing an external energy supply enabling the integration of some system sensors to control the structure's damping response. In some cases, an external real-time data acquisition is required for providing a more efficient and accurate active response of the attached mechanism, presenting itself as a solution that entails more costs and maintenance work. Furthermore, all this equipment means additional mechanical organs and with it, more weight

and complexity to the system. Although it is the best and only damping solution for some specific cases, many sectors are searching for alternatives capable to maintain the same safety factors and load requirements. Therefore, there are plenty of situations where passive control is the most effective and efficient way to reduce weight, costs, maintenance works and, furthermore, less probably of system's failure. However, passive damping is not capable of instant feedback capability in response to a specific stimulus, which implies an automatic adjustment to the required level. Thereby, active control systems remains the best solution to measure specific external inputs and provides an instant feedback response, allowing a continuous desired level of damping, as exemplified in Figure 2.

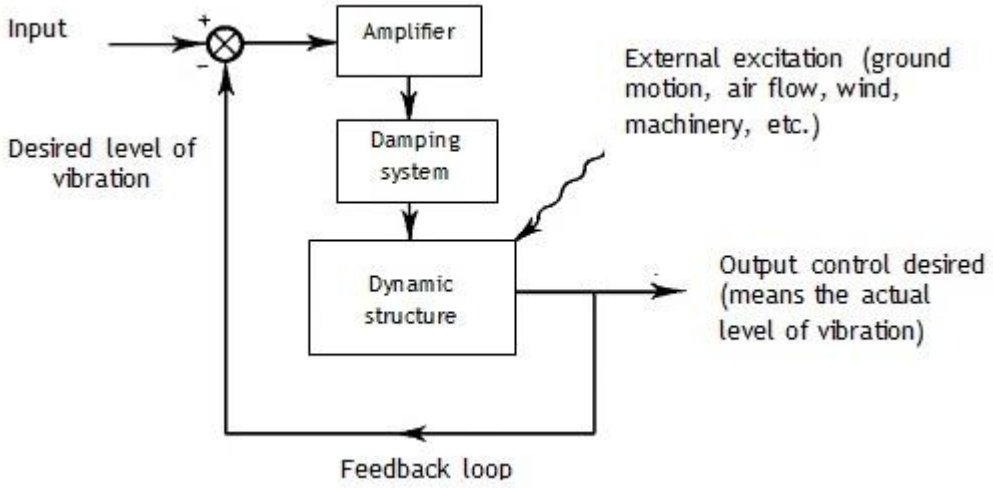

Figure 2 – Example flowchart of an active damping system.

Passive control

It is clear that there are added costs and complexity with active systems compared to passive control solutions. Passive control refers to energy dissipation based on the use of passive technologies (such as structural joints, supports and isolators) or by integrating a damping material (such a viscoelastic layer) in a host structure, providing internal damping. Passive damping treatments are less expensive to produce than other methods, but their successful application requires a complete understanding of the vibration problem and the properties of the damping candidate materials. Viscous dampers, dynamic absorbers, shunted piezoceramics dampers, and magnetic dampers are other mechanisms of passive vibration control. This type of control is used to eliminate unwanted dynamics in the structure and to achieve a reduction of system disturbance excitation with specific and precise control of some parameters, increasing the overall structural stability. Table 1 presents a short compilation of some damping category materials performance and their pros and cons in passive or active control.

Table 1 –Active vs passive damping: advantages and disadvantages.

Damping material		Advantages	Disadvantages
Passive damping	Viscoelastic	• High Damping • Low weight penalty • No external energy needed • Low costs in production or operation	• Unsuitable for very low and high temperatures and at low frequencies • No controllability
	Hard damping alloys	• High temperature, high frequency operating range • No external effort needed	• Relatively low damping • High weight penalty • High strain dependency • No controllability
Active damping	Piezoelectric, magnetostrictive alloys or composites	• Controlled blocking force generation • High or Moderate temperature, high frequency operating range	• Low inherent damping in most operating ranges • External energy supply • Instability issues in control
	Shape Memory alloys	• Large strain applications	• Lower controllability • Low frequency bandwidth • Needs either stress or temperature induced phase transformation

2.2 Introduction to viscoelastic materials

2.2.1 Basic concepts

As referred before, a viscoelastic material is an efficient solution for passive damping treatments. Such materials exhibit both viscous and elastic behaviour, and their properties are influenced by different parameters, namely load, time, temperature and frequency. This type of materials dissipate vibrational energy in the form of heat that is generated when the material is stressed by deformation, mostly in shear motion. In general, these materials have low shear modulus values but high loss factors, being the damping characterized by the complex modulus translated into a complex stiffness matrix.

Based in this concept, the application of these materials as a straightforward solution for vibration suppression is presented with a myriad of possible configurations and modifications that can be explored in order to develop new damping solutions for diverse industrial applications. Table 2 illustrates some of the most used viscoelastic materials in engineering

applications, which can be divided in polymers, rubbers, pressure sensitive adhesives, urethanes, epoxies and enamels.

Table 2 – Most common viscoelastic materials used for damping purposes. [16]

Acrylic Rubber
Butadiene Rubber (BR)
Butyl Rubber
Chloroprene
Chlorinated Polyethylenes
Ethylene-Propylene-Diene
Fluorosilicone Rubber
Fluorocarbon Rubber
Nitrile Rubber
Natural Rubber
Polyethylene
Polystyrene
Polyvinyl Chloride (PVC)
Polymethyl Methacrylate (PMMA)
Polybutadiene
Polypropylene
Polyisobutylene (PIB)
Polyurethane
Polyvinyl Acetate (PVA)
Polyisoprene
Styrene-Butadiene (SBR)
Silicone Rubber
Urethane Rubber

2.2.2 Viscoelastic materials behaviour

Viscoelastic materials have the particularity of possessing both viscous and elastic behaviour. Hooke's law applies to elastic materials, where the stress is proportional to the strain and the Young's modulus is defined as the stress to strain ratio. Figure 3 shows the distinct behaviour of viscoelastic and elastic stress-strain curves in time domain, where σ is the applied stress, ε the respective strain and ω the loading frequency (which is out-of-phase with strain by some angle ϕ). In fact, ϕ could be a measure of the materials damping capability. Considering an elastic material, the curves illustrate that all the energy stored during loading is returned when the load is removed, resulting in an in-phase stress-strain behaviour. Viscoelastic materials, on the other hand, exhibit a time dependent relationship between stress and strain, which means that the slope of the stress-strain plot depends on strain rate. For a viscoelastic material, the modulus is represented by a complex quantity with real and imaginary parts. For small stress excitation the viscoelastic materials reaction can be described by a linear viscoelastic behaviour, and due to the correspondence principle, the Young's modulus and shear modulus can be treated as complex quantities, where the real part is known by *Storage modulus* and the imaginary part by *Loss modulus*, this latter defining the energy dissipative ability of the material [4].

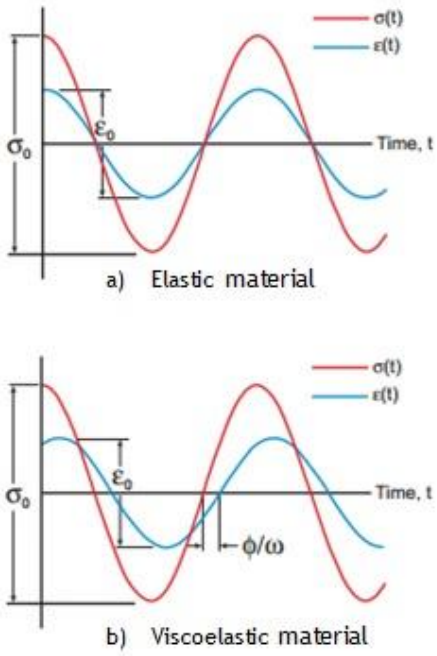

Figure 3 – Elastic versus Viscoelastic material strain behaviour in time domain during cyclic stress loading: a) For an elastic material; b) For a viscoelastic material.

More precisely, the viscoelastic time dependency contrasts with common elastic materials, whose behaviour is not time dependent. The stiffness and strength of materials is frequently illustrated by a stress–strain curve as exemplify in Figure 4 for both viscoelastic and elastic-plastic materials. When the material is linearly elastic, its behaviour is typically a straight line with a slope proportional to the Young's modulus. For a sufficiently large stress, the elastic material exhibits a threshold stress, the yield stress σ_y. However, in the viscoelastic curve both time and strain increase together. Thus, viscoelastic materials strain-stress analysis reveal the typical behaviour shown with more detail in Figure 5. For such type of materials, energy is stored during the loading cycle, whereas during the unloading phase the energy recovery follows the pattern shown in Figure 5, where the shaded region is a measure of the energy lost due to heat transfer mechanisms during deformation. Moreover, it is well known that the area beneath a stress-strain curve is the energy per unit volume. Therefore, when the load is removed, viscoelastic materials exhibit a time delay in returning the material to its original shape, which comes from the energy loss mechanisms.

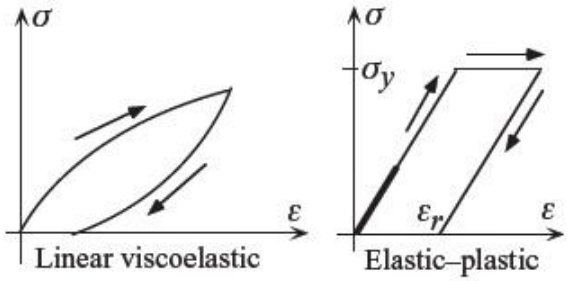

Figure 4 - Stress–strain plots comparison for viscoelastic and elastic-plastic materials under constant strain rate [20].

When this type of material is submitted to a load condition, part of the deformation induced by shear stressing has an elastic nature and will return to zero when the force is removed. The other part of deformation will not return to zero when the force is removed because the elastic displacement remains constant, whereas the sliding displacement continues, with tendency to increase. This is the description for viscoelastic capacity to both store and dissipate mechanical energy [17, 18]. Furthermore, the viscoelastic response depends on all past states of stress and strain, which confers a "memory" capacity according to all previous stress conditions applied to the material [19].

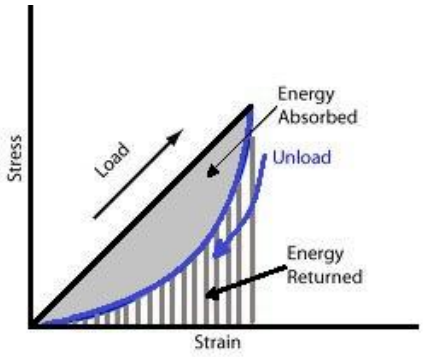

Figure 5 – Typical stress-strain behaviour in viscoelastic materials.

Commonly, a creep recovery test is used to characterize such memory capacity from the dynamic response. Figure 6 illustrates a typical viscoelastic curve response resulting from a creep-recovery test. The dynamic response is said to exhibit both an instantaneous elasticity effect and creep characteristics; therefore, as it can be seen, this behaviour is not fully described by either considering the elasticity or viscosity theory sole effect, but from the combination of features from each of these theories.

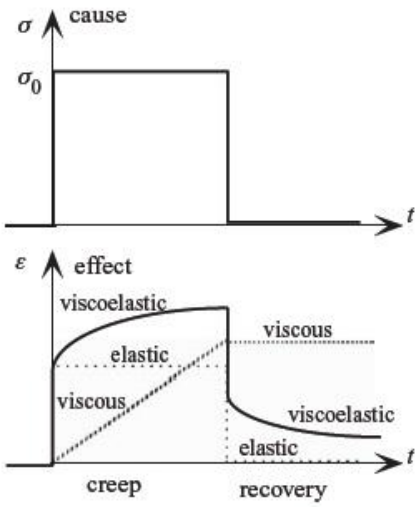

Figure 6 - Typical viscoelastic curve response resulting from a creep-recovery test [20].

Analytically, the relationship between shear stress, elastic stress and viscous stress can be described in terms of a complex number " i " (i=$\sqrt{-1}$) . Thereby, the real part of a complex modulus represents the elastic portion and the imaginary part represents the viscous portion of the material response. The elasticity and viscosity components of viscoelastic materials are often described by a relation using Young's modulus E and Poisson's ratio ν of the material. These relations count both longitudinal and transverse response so that E and υ could be calculated as described in equations (2.1) and (2.2) [20, 21]:

$$E = \frac{9GK}{3K + G} \tag{2.1}$$

$$\upsilon = \frac{3K - 2G}{6K + 2G} \tag{2.2}$$

Where G is the shear modulus and K is the bulk modulus. However, for a complete characterization of the viscoelastic behaviour it is more convenient to use the complex shear modulus G^* and complex bulk modulus K^* rather than E and υ, which in turn can be obtained by using relations valid for homogeneous, isotropic and linear solid viscoelastic materials. Thus, a complete description of the viscoelastic behaviour can be obtained from equations (2.3) and (2.4). Similarly, Poisson's ratio and Young's modulus are complex parameters given by equations (2.5) and (2.6). Thus, in the following equations G' is the storage shear modulus, G'' is the loss shear modulus, K' is the storage bulk modulus, K'' is the loss bulk modulus, G_0 is the instantaneous shear modulus, K_0 is the instantaneous bulk modulus, υ' is the Poisson's

dynamic ration, v'' is the Poisson's loss ratio, E' is the storage Young's modulus and E'' is the loss Young's modulus.

$$G^*(\omega) = G'(\omega) + iG''(\omega) \tag{2.3}$$

$$K^*(\omega) = K'(\omega) + iK''(\omega) \tag{2.4}$$

$$v^*(\omega) = v'(\omega) + iv''(\omega) \tag{2.5}$$

$$E^*(\omega) = E'(\omega) + iE''(\omega) \tag{2.6}$$

Energy storage and dissipation cannot be negative, so both real and imaginary parts of a complex modulus have to be non-negative. Regarding the Poisson's ratio in viscoelastic materials, many studies account for the difference between Poisson's ratios in creep and in relaxation and its time dependence, concluding that the difference is minor unless there is a large relaxation strength. In this case, Poisson's ratio is assumed constant in time for low-density materials, especially honeycombs and foams [23]. This will be the assumption for the definition of the cork properties in the numerical model described in this work. Furthermore, given E^* and v^* , it is possible to determine both the complex shear modulus(G^*) and complex bulk modulus (K^*) by using the following expressions [22, 24] :

$$G^* = \frac{E^*}{2(1+v^*)} \tag{2.7}$$

$$K^* = \frac{E^*}{3(1-2v^*)} \tag{2.8}$$

The most widespread theory used to model polymers (including FRPs) is based in theory of linear viscoelasticity which describes that, at any given time and for small strain, there is a linear relationship between stress and strain. Any linear viscoelastic material behaviour may be represented by a hereditary approach based on the Boltzmann superposition principle, which will be analysed ahead in this work.

Temperature effects on viscoelastic behaviour

Polymeric materials widely used as damping treatments are more sensitive to temperature than general metals, plastics or composite materials. Viscoelastic properties, such as the complex modulus, present three main temperature regions of interest, namely the glassy

region, transition region, and rubbery region [16, 25, 26]. Low temperatures are represented by the glassy region where the storage modulus is generally much higher than that for the transition or rubbery regions. This region can be defined by different temperature values for different materials depending on the viscoelastic composition. Figure 7 illustrates the behaviour of the complex shear modulus and loss factor in the different temperature regions. For the glassy region, loss factor is characterized by small values due to the high storage modulus dimension. Thus, in this region, the viscoelastic material presents high stiffness being unable to deform at the same magnitude (per unit load) as it would operate in the transition or rubbery regions (where the material is softer). Hence, for high operation temperatures, viscoelastic materials present low storage moduli and, consequently, low stiffness. That low value is typical of the rubbery region where the loss factor is equally smaller due to the increasing structural breakdown of material as the temperature is increased being the viscoelastic material easily deformable. Devices as isolators or tuned mass dampers are the most appropriate to be used in this region of temperature because the shear modulus is nearly constant.

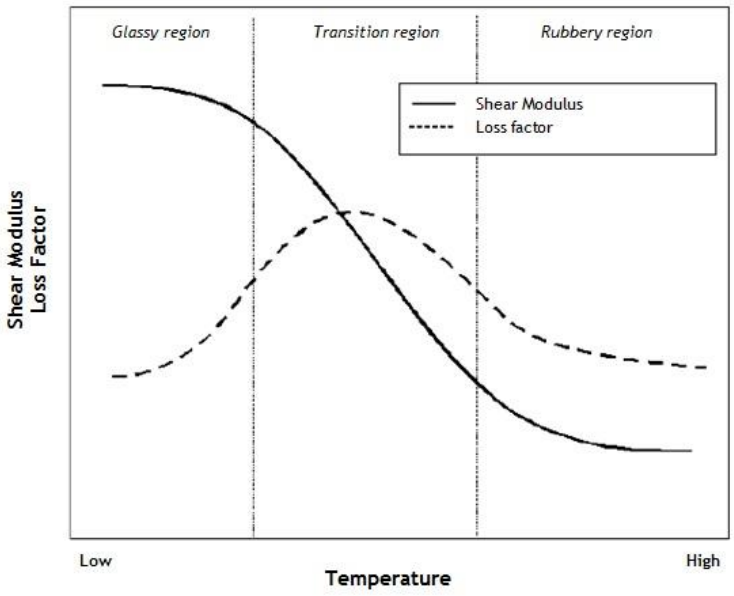

Figure 7 - Temperature effects on complex modulus and loss factor.

In the context of the present work, the most important region relies between the glassy and rubbery regions, known as transition region. Due to the fact that the maximum loss factor value is reached in this region, applications with viscoelastic materials for damping purposes generally should be used within the transition temperature range. Here, frictional molecular effects result in the increase of the mechanical damping characteristic of viscoelastic materials. Therefore, knowing the operating temperature range during the design phase of a host structure to which a viscoelastic damping treatment will be applied will be determinant to optimizing the damping effectiveness of the whole system.

Frequency effects on viscoelastic behaviour

As for the temperature effect described in the last section, frequency variation also has a significant effect in the complex modulus properties of a viscoelastic material. As Figure 8 shows, frequency has an inverse relationship to complex shear modulus when compared with temperature, since the storage modulus and the loss factor are small at low frequencies. This is due to the low cyclic strain rates within the viscoelastic layer. As the frequency increases, the material converges to the transition region where the loss factor reaches a maximum value. With a further frequency increase, the storage modulus raises but loss factor decreases. As it happens with the temperature dependence, the transition region is the typical operating frequency range for loss factor maximization [27-29].

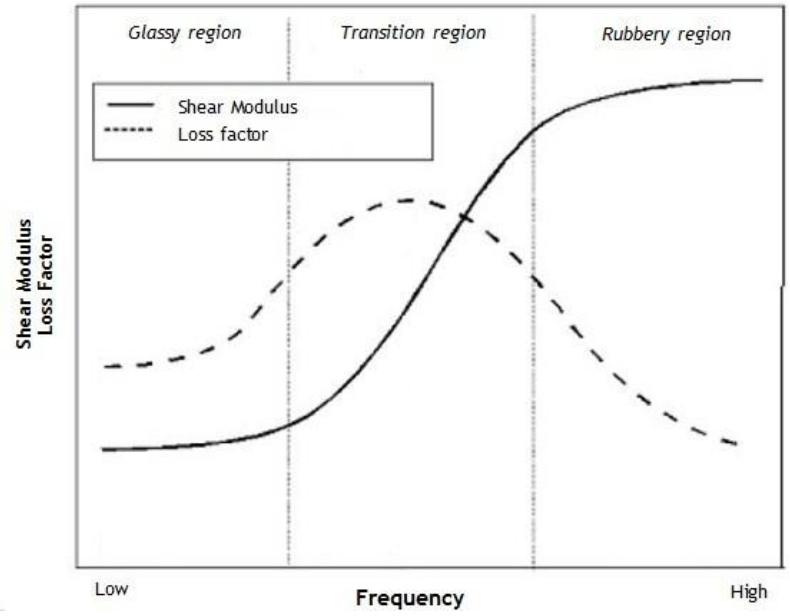

Figure 8 - Frequency effects on complex modulus and loss factor

2.2.3 Linear viscoelasticity response: Mathematical models

Viscoelastic behaviour can be represented using mathematical models based on spring and dashpot elements corresponding to the elastic and viscous responses, respectively (as illustrated in Figure 9). Aiming at simplifying the analysis of this type of material, linear theory models are the most successful widespread methods, supporting extrapolation or interpolation of experimental data, reducing complex approximations and time-consuming

calculations. The description of a viscoelastic model can be resumed by considering the elastic and viscous terms formulated in equations (2.9) and (2.10), respectively:

$$\sigma = E\,\varepsilon \tag{2.9}$$

$$\sigma = \mu\,\dot{\varepsilon} \tag{2.10}$$

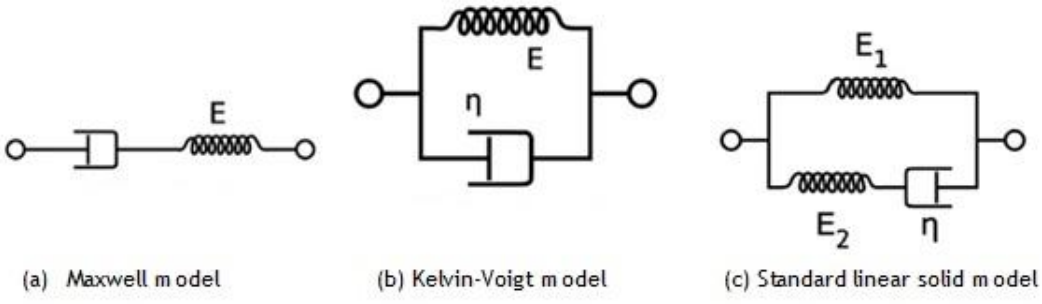

Figure 9 - Mathematical models for viscoelastic response

The elastic term is modelled as springs and the other term, the viscous component, as dashpots. E represents the Young's modulus, μ is the viscosity of the material, ε the correspondent strain and $\dot{\varepsilon}$ is the strain rate. Instantaneous inherent deformations of the material are modelled like a spring response with a magnitude related to the fraction of mechanical energy stored reversibly as strain energy. The entropic uncoiling process is fluid like some cases in Nature, and can be modelled by a Newtonian dashpot. The main models used to describe the viscoelasticity in materials are listed below.

The Maxwell model

This model consists of an elastic spring in series with a viscous dashpot. When the ends are pulled apart with a certain force, the stress on each element is the same and equal to the imposed stress, as described in equation (2.11).

$$\sigma = \sigma_{spring} = \sigma_{dashpot} \tag{2.11}$$

The total strain rate is equal to the sum of the spring rate and the dashpot rate, and the absolute total strain can be divided in the strain in each element, as described in equation

(2.12). In a simplistic way, Maxwell model is usually applied in cases with small deformations. Instead, large deformations should include some geometrical non-linearity. The model characterizes a general material response under a constant strain, where the stresses gradually relax, and under a constant stress, where the strain can be divided in both elastic and viscous components. The elastic response occurs instantaneously, corresponding to the spring elastic contribution, and relaxes immediately upon stress release assumed by the viscous component which grows with time as long as the stress is applied.

$$\varepsilon = \varepsilon_{spring} + \varepsilon_{dashpot} \tag{2.12}$$

By differentiating the strain equation and writing the spring and dashpot strain rates in terms of the stress, the following equations can be obtained:

$$\dot{\varepsilon} = \dot{\varepsilon}_{spring} + \dot{\varepsilon}_{dashpot} = \frac{\dot{\sigma}}{k} + \frac{\sigma}{\mu} \tag{2.13}$$

$$\dot{\varepsilon} = \dot{\varepsilon}_{spring} + \dot{\varepsilon}_{dashpot} = \frac{1}{E}\dot{\sigma} + \frac{\sigma}{\mu} \tag{2.14}$$

Where k is the elasticity constant of the spring, σ is the stress and μ is the material's viscosity. In Maxwell model, stress decays exponentially with time, a well-known phenomenon for most polymers; however, its creep response prediction is difficult and limited. Additionally, at creep or even at constant-stress conditions, this model shows that strain will increase linearly with time, assuming that for most polymers cases the strain rate decreases with time [21, 30].

The Kelvin-Voigt model

This model can be represented by a Newtonian damper and a purely elastic spring connected in parallel. Thus, this model can be viewed as a mixture of a linearized elastic solid and a linearly viscous fluid that co-exist, where the constitutive relation is a sum of the two terms. Hence, the total stress will be the sum of the stress in each component [31]:

$$\sigma = \sigma_{spring} + \sigma_{dashpot} \tag{2.15}$$

$$\sigma = E\varepsilon + \mu\,\dot{\varepsilon} \tag{2.16}$$

Another fact is that since the two components of the model are arranged in parallel, the strains in each component are the same:

$$\varepsilon = \varepsilon_{spring} = \varepsilon_{dashpot} \tag{2.17}$$

For a situation with constant stress, Kelvin-Voigt model describes that a material deforms at a decreasing rate, approaching asymptotically the steady-state strain. Although the model does not accurately describe stress relaxation, dynamic response is characterized by a gradual relaxation to its undeformed state [30]. However, only certain thermoplastics with low degree of cross-linking will deform accurately according to this model.

The standard linear solid or Zener model

This model offers more realistic representation of the material's behaviour over the whole frequency range from creep and stress relaxation to dynamic modulus, dynamic loss factor, rate effects and impact loading. It uses a linear combination of springs and dashpots, which basically consists in adding a spring in parallel with the Maxwell model. Since the Maxwell model does not describe creep or recovery, and the Kelvin–Voigt model does not describe stress relaxation, the standard linear solid is the simplest model capable to predict both [32]. Taking into consideration changes in stress and strain at the same time, the general viscoelastic behaviour in equilibrium can be summarized as:

$$\sigma = E\,\varepsilon + \mu\,\dot{\epsilon} \tag{2.18}$$

$$\sigma + \frac{\mu}{E_m}\varepsilon = E_a\varepsilon + (E_a + E_m)\frac{\mu}{E_m}\dot{\varepsilon} \tag{2.19}$$

Where σ is the true stress, ε is the true strain, E_m the spring Young's modulus in series with the dashpot and E_a the parallel spring Young's modulus. Therefore, at stress relaxation, the strain is held at a constant value, thereby implying that the term ($\dot{\varepsilon}$) is zero.

The Boltzmann superposition integral

Remembering that in the dynamic response of a viscoelastic material, internal stresses are a function not only of the instantaneous deformation but also depend on the strain past history. Therefore, the most recent past history has more influence fostering the linear viscoelasticity as the simplest way to model the response of such materials. With the Boltzmann superposition principle, the current stress is determined by the superposition of the responses, using the strain increment. Let's consider the function $\Omega(t)$ representative of some shear strain acting on a viscoelastic material and $\sigma(t)$ as the shear stress (which represents the effect resulting from the shear strain). A variation in shear strain occurring at time t_A will influence the effect some time later, which can be expressed by equation (2.20). Thus, for linear isotropic viscoelasticity response, the basic hereditary integral formulation is given by equation (2.21):

$$\sigma(t) = G(t - t_A)\ \delta\ \Omega(t_A) \tag{2.20}$$

$$\sigma(t) = \int_0^t 2G(\tau - \tau')\dot{e}dt' + I \int_0^t 2G\ (\tau - \tau')\ \dot{\phi}\ dt' \tag{2.21}$$

$$\frac{d\tau}{dt} = \frac{1}{A_\theta(\theta(t))'} \tag{2.22}$$

$$\tau = \int_0^t \frac{dt'}{A_\theta(\theta(t'))} \tag{2.23}$$

Being $\dot{e}$ and $\dot{\phi}$ the mechanical deviatoric and volumetric strains, K is the bulk modulus and G is the shear modulus, functions of the reduced time τ. This reduced time parameter is related to the actual time through the integral differential equation described in equations (2.22) and (2.23). In equation (2.20), $G(t - t_A)$ represents a relaxation function or relaxation modulus, which is a function of the time delay between cause and effect, known as independent of the strain amplitude, which represents the "fading memory" mentioned before. For equations (2.22) and (2.23), θ is the temperature and A_θ is the shift function (Williams-Landel-Ferry [WLF] equation is the most used shift equation), highly related with the temperature dependence of viscoelastic materials. The FEM software ABAQUS® used in this work allows the WLF equation to be used with any convenient temperature, for instance a reference temperature. Therefore, note that if $A_\theta = 1,\ \tau = t$ [33].

Regarding the vibration analysis of a composite material, general structural vibration can be measured using electronic sensors which convert vibration motion into electrical signals.

These signals can be considered either in time or frequency domains, depending on the type of information required for the analysis of results. Any time history signal can be transformed into the frequency domain using a Fourier transform, which requires some complex math. However, today's signal analysers, as the one used in this work's experimental testing, race through it automatically in real-time conditions.

As it will be seen in chapter 4, the applied load used for the dynamic excitation of the composite beam under analysis in this work is small. Considering a shear test at small strain, in which a time varying shear strain, ε_t, is applied to the material, the respective viscoelastic response is the shear stress, $\tau(t)$, described as:

$$\tau(t)= \int_0^t G_R(\tau - s)\dot{\varepsilon}(s)ds \tag{2.24}$$

G_R is the time dependent shear relaxation modulus, whose respective behaviour can be illustrated by considering a relaxation test where a strain ε is suddenly applied and held constant for a long time. For the initial condition t=0 and considering a fixed strain ε, then:

$$\tau(t)= \int_0^t G_R(\tau - s)\dot{\varepsilon}(s)ds = G_R\,\varepsilon \quad (\text{since } \dot{\varepsilon} = 0 \; for \; t > 0) \tag{2.25}$$

Since the viscoelastic material model is long-term elastic, the response tends to a constant stress ($G_R(t) \rightarrow G_\infty$ as t $\rightarrow \infty$) after a constant strain has been applied for a long time. Resorting to the instantaneous shear modulus, $G_0 = G_R(0)$, the shear relaxation modulus can be written in a dimensionless form, as expressed in equation (2.26). Hence, the stress expression can be formulated like in equation (2.27):

$$g_R(t) = \frac{G_R(t)}{G_0} \tag{2.26}$$

$$\tau(t)= G_0 \int_0^t g_R(\tau - s)\dot{\varepsilon}(s)ds \tag{2.27}$$

2.2.4 Viscoelastic frequency dependence: numerical model

The dissipative part of the material dynamic response is defined by using the real and imaginary parts as function of frequency (for compressible materials). ABAQUS® allows to model the viscoelastic behaviour as a function of frequency in three different ways: by using

a power law, given an experimental tabular input, or by a Prony series expression for the shear and bulk relaxation moduli. In the ABAQUS® solver, the viscoelastic material is defined by a Prony series expansion of the dimensionless relaxation modulus [33]:

$$g_R(t) = 1 - \sum_{i=1}^{X} \overline{g_i^P} \ (1 - e^{\frac{-t}{\tau_i^G}}) \tag{2.28}$$

$$k_R(t) = 1 - \sum_{i=1}^{X} \overline{k_i^P} \ (1 - e^{\frac{-t}{\tau_i^G}}) \tag{2.29}$$

Where X, $\overline{g_i^P}$, $\overline{k_i^P}$, τ_i^G, i=1,2,...,X are material constants.

During the numerical analysis, the solver will automatically perform the conversion between time and frequency domains. The time-dependent shear modulus can be obtained from the following expressions [33]:

$$G'(\omega) = G_0 \left[1 - \sum_{i=1}^{X} \overline{g_i^P}\right] + G_0 \sum_{i=1}^{X} \frac{\overline{g_i^P}\ \tau_i^2\ \omega^2}{1 + \tau_i^2\ \omega^2} \tag{2.30}$$

$$G''(\omega) = G_0 \sum_{i=1}^{X} \frac{\overline{g_i^P}\ \tau_i\ \ \omega}{1 + \tau_i^2\ \omega^2} \tag{2.31}$$

$$K'(\omega) = K_0 \left[1 - \sum_{i=1}^{X} \overline{k_i^P}\right] + K_0 \sum_{i=1}^{X} \frac{\overline{k_i^P}\ \tau_i^2\ \omega^2}{1 + \tau_i^2\ \omega^2} \tag{2.32}$$

$$K''(\omega) = K_0 \sum_{i=1}^{X} \frac{\overline{k_i^P}\ \tau_i\ \ \omega}{1 + \tau_i^2\ \omega^2} \tag{2.33}$$

Where G' is the storage shear modulus, G'' is the loss shear modulus, K' is the storage bulk modulus, K'' is the loss bulk modulus, $G_0$is the instantaneous shear modulus and K_0 is the instantaneous bulk modulus.

Since it was assumed that dissipative losses acting in the analysed specimens were mainly caused by internal damping ("viscous") effects, the frequency domain was adopted for the analysis of the viscoelastic material, describing frequency-dependent material behaviour in small steady-state harmonic. Thus, it was assumed that the shear (deviatoric) and volumetric behaviours are independent in multiaxial stress states. Therefore, the tabular form was used to model the dynamic motion of cork in ABAQUS® software. This was defined by giving the real and imaginary parts of ωg^* and ωk^* as functions of frequency in cycles per time, being ω the circular frequency. The real and imaginary parts of ωg^* and $\omega k^*$are given by [24]:

$$\omega\, \Re(g^*) = \frac{G_l}{G_\infty} \tag{2.34}$$

$$\omega\, \Im(g^*) = 1 - \frac{G_s}{G_\infty} \tag{2.35}$$

$$\omega\, \Re(k^*) = \frac{K_l}{K_\infty} \tag{2.36}$$

$$\omega\, \Im(k^*) = 1 - \frac{K_s}{K_\infty} \tag{2.37}$$

Where $G_\infty$and K_∞ are the long-term shear and bulk modulus determined from the elastic or hyperelastic properties.

2.2.5 Vibration theory applied to viscoelastic materials

Structural mechanical vibrations can be subdivided according to the vibration sources or the systems' constituents. On the other hand, vibration phenomena may occur in many areas of mechanical, civil and aerospace engineering.

The general response of a mechanical system, with *n* degrees of freedom, can be represented by the next equation:

$$\mathrm{M}]\ddot{X} + \ [\mathrm{C}]\dot{X} \ + \ [\mathrm{K}]X = \ [\mathrm{F(t)}] \tag{2.38}$$

In this equation, the terms [M], [C], [K] are the mass, damping and stiffness system matrices, respectively; [F(t)] is the external load vector to be considered in the numerical model; $\ddot{X}$, $\dot{X}$ and X are the acceleration, velocity and generalised displacement vectors, respectively. In a vibrating structure, the system's parameters are used to create the mathematical model, in which the mass and stiffness can be derived as a function of the system's geometry and material characteristics. In terms of finite element formulation, and considering a harmonic vibration, the equilibrium equations can be described by:

$$\big[[K(\omega)] - \ \omega^2\ [M]\big]\{U\} = [F(t)] \tag{2.39}$$

The harmonic response assumes the form:

$$\{U\} = \emptyset\, e^{i\,\omega t} \tag{2.40}$$

Where $\emptyset$ represents all eigenvectors of each vibration mode, ω the frequency value and t the time domain. Now, by replacing equation (2.40) in (2.39) we will get:

$$\left[[K] - \omega^2\,[M]\right]\emptyset\, e^{i\,\omega t} = [F(t)] \tag{2.41}$$

Considering vector [F(t)] = 0, and noting that $e^{i\,\omega t}$ cannot be equal to zero, equation (2.41) assumes the form:

$$\left[[K(\omega)] - \lambda\,[M]\right]\emptyset = [0] \tag{2.42}$$

In equation (2.42), λ is ω^2 and represents the eigenvalues of the system. So if $\lambda = \omega^2$, the solution of this expression corresponds to a conventional eigenvalue problem and has a correspondent eigenvector $\emptyset$ that represents the system modes of vibration [12]. Thus, for a general damping system, the damped natural frequencies (ω_d) are given by:

$$\omega_d = \omega_{und}\sqrt{1-\xi^2} \tag{2.43}$$

Where ω_{und} and ξ are the undamped natural frequency and the damping ratio, respectively.

From the numerical model using a conventional finite element code it is possible to determine the system's mass and stiffness matrices. On the other hand, damping can be simulated from the mathematical theory concerning the Rayleigh damping model, where the energy dissipation of the system can be expressed by a damping matrix [C] with symmetric coefficients. In this model, the symmetric damping matrix [C] is a linear combination of the mass and stiffness matrixes of the system. Therefore it can be defined as:

$$[\mathrm{C}] = \alpha\,[\mathrm{M}] + \beta\,[\mathrm{K}] \tag{2.44}$$

$$\alpha + \beta\omega_i^2 = 2\omega_i\xi_i \tag{2.45}$$

In equation (2.44), α is the mass proportional damping factor and β is the stiffness proportional damping factor. Both have an important role in modelling damping, where α and β are the attributes of the lower and higher natural frequencies, respectively. In equation (2.45) ω_i is the natural frequency obtained through modal analysis and ξ_i the respective modal damping ratio. Pointing out that the structural component developed in this work will typically operate at relative low frequencies (for example, for space applications or low frequency noise control) it is assumed that $\beta \ll 1$, resulting in higher structural dependency of α value. Therefore, relating equations (2.42), (2.43) and (2.45) allows concluding that the mass proportional damping factor and the stiffness proportional damping factor can assume the form:

$$\alpha_i = \omega_i\sqrt{1-\xi_i^2} \quad and \quad \beta_i = \omega_i\,\xi_i \tag{2.46}$$

Thus,

$$\alpha_i = 2\,\omega_i\xi_i \quad \text{or} \quad \alpha_i = \omega_i\,\eta_i \tag{2.47}$$

$$\xi_i = \frac{\alpha_i}{2\,\omega_i} + \frac{\beta\,\omega_i}{2} \tag{2.48}$$

$$\beta_i = \frac{2}{\omega_i}\left(\xi_i - \frac{\alpha_i}{2\,\omega_i}\right) \tag{2.49}$$

In the abovementioned equations, for a given *ith* vibration mode, ω is the damped natural frequency, ξ the damping ratio and η the loss factor. In a dynamic analysis relying upon a finite element model, damping is related with these α and β parameters, which directly affect the damping ratio, and consequently, the loss factor. Given that, for numerical purposes, the mass coefficient (α) is an input and should be based on experimental data obtained for the particular specimen geometry and types of materials considered in this analysis.The elastic and viscous stresses are related to the material properties through the storage modulus, which represents a ratio of stress to strain (if elastic stresses are considered) or loss modulus (in the case of considering viscous stresses) [4].

2.3 Damping on Sandwich structures with constrained layer

Due to the importance of layered composites in a wide range of industrial and aerospace applications and its increasing investment prospective, the vibration control of layered composites has been an area of fundamental research over the past fifty years. The sandwich structure solution depends on variable parameters, such as the skin, core layers and adhesive attachment in the interface regions [34]. The separation of the outer faces by the core increases the moment of inertia of the panel with little increase in weight, producing an efficient structure for resisting bending and buckling loads. Normally, sandwich structures are fabricated by attaching two thin stiff skins as laminate covers, a lightweight core with variable thickness to separate those skins and carry the loads between them, which in turn are joined by an adhesive element capable of transmitting shear and axial loads to and from the core [35]. Figure 10 illustrates some of the types of cores used in sandwich composite structures.

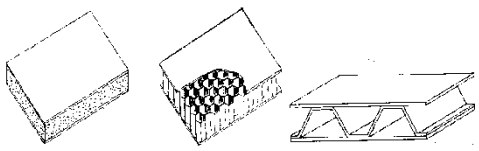

(a) Foam (b) Honeycomb (c) Corrugated

Figure 10- Types of cores used in sandwich components [34].

Ross, Kerwin and Ungar (RKU) [35] made a pioneering work consisting in modelling a three-layer sandwich beam to predict damping in plates with embedded damping layer. The first theoretical approach was presented by Kerwin regarding damped thin structures with a constrained viscoelastic layer. This author concluded that the energy dissipation mechanism in the constrained core is attributed to its shear motion, and as such the viscoelastic core was represented by a complex modulus. Furthermore, the sandwich based upon Euler-Bernoulli beam theory, known as Mead and Markus model, disregards the longitudinal and rotational inertia from the outer layers, but it only includes transverse inertia and shear effects in the central core layer (i.e., longitudinal momentum, bending and extensional stresses are ignored in the core). Rao and Nakra included these same effects in their equation of motion using the energy method [36-38]. These are the most widespread basic theories and models for a layered sandwich beam with a viscoelastic material core, although most of them neglect the effect of shearing in the skins.

2.3.1 Ross-Kerwin-Ungar damping model

The damping model developed by Ross, Kerwin and Ungar [35] is mainly used for three layered sandwich beams based on damping resulting from flexural waves induced by a constrained viscoelastic layer, although some modifications can adapt the model to more general applications regarding any sandwich type laminate. This model is based upon their researches in which the dynamic material properties of viscoelastic materials can be extracted from measurements made on composite beams or even on other homogenous materials through the application of the RKU equations, which is presented as the simplest, most readily used, and often the most reliable approach. As many models, the RKU model accounts for several assumptions that can be extrapolated to any other constrained layer damping treatment applied to a rectangular beam, namely:

- For the entire composite structure cross section, there is a neutral axis whose location varies with frequency;
- There is no slipping between the elastic and viscoelastic layers at their interfaces;
- The major part of damping is due to the shearing of the viscoelastic material, whose shear modulus is represented by complex quantities in terms of real shear moduli and loss factors;
- The elastic layers have the same amount of lateral displacement;
- The beam is simply supported and vibrating at a natural frequency (or the beam is infinitely long so that the end effects may be neglected).

Figure 11 represents a typical sandwich system with an embedded viscoelastic layer and stacking sequence that can be defined for analysis proposes. The flexural rigidity (EI) of such system can be formulated as indicated in equation (2.50):

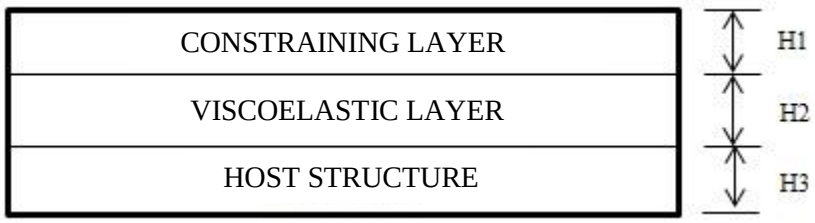

Figure 11- Schematic representation of the sandwich laminate considered for the analytical analysis.

$$EI = \frac{E_1 H_1^3}{12} + \frac{E_2 H_2^3}{12} + \frac{E_3 H_3^3}{12} + E_1 H_1 D^2 + E_2 H_2 (H_{21} - D)^2 + E_3 H_3 (H_{31} - D)^2 - \left[\frac{E_2 H_2^3}{12} + \frac{E_2 H_2}{2}(H_{21} - D) + E_3 H_3 (H_{31} - D)\right] \frac{H_{31} - D}{1 + g} \quad (2.50)$$

Where:

$$D = \frac{E_2 H_2 \left(H_{21} - \frac{H_{31}}{2}\right) + g(H_{21} E_2 H_2 + H_{31} E_3 H_{31})}{H_1 E_1 + \frac{E_2 H_2}{2} + g(E_1 H_1 + E_2 H_2 + E_3 H_3)} \quad (2.51)$$

$$H_{31} = \frac{H_1 + H_3}{2} + H_2 \quad (2.52)$$

$$H_{21} = \frac{H_1 + H_2}{2} \quad (2.53)$$

$$g = \frac{G^* L^2}{(H_2 H_1 E_1 \sqrt{C_n \zeta_n})} \quad (2.54)$$

$$\zeta_n = \sqrt{\frac{\rho_{CFRP} H_1^2 \omega_n^2 L^4}{E_3 I_1}} \quad (2.55)$$

$$I_1 = \frac{H_1^4}{12} \quad (2.56)$$

E= Young's modulus [Pa];

G=Shear Modulus [Pa];

H= Layer Thickness [m];

G^* = Complex shear modulus;

L= Length of the laminate;

g = Shear parameter;

C_n = Correction factor (defined in table 3)

ρ_{CFRP} = CFRP's density [Kg/m^3];

ω_n = Natural frequency [rad/s];

Table 3 - Rao correction factors for shear parameter in RKU equations [16].

Boundary conditions	Correction factors	
	Mode 1	*Mode 2*
Pined-pined	1	1
Clamped - clamped	1.4	1
Clamped - pined	1	1
Clamped - free	0.9	1
Free - free	1	1

Therefore, the loss factor of a system with an embedded viscoelastic layer can be found from the ratio of the imaginary and real parts of *EI*, as shown in equation (2.57) [39]. Thus, η_{RKU} (equation (2.57)) is the estimated loss factor obtained from the application of the RKU equations:

$$\eta_{RKU} = \frac{Imag\ (EI)}{Real\ (EI)} \tag{2.57}$$

2.3.2 Direct frequency response technique

The solution presented by Sun, Sankar and Rao [40] based on the direct frequency response technique developed by C.D Johnson, D.A Kienholz et al. is another option to estimate the structural loss factor value. These authors used it for analytical estimation of damping in beams under forced vibration. This technique presents itself as a simply and fast method to estimate the modal loss factor from the real part of the response, as explained in Figure 12 and equation (2.58).

$$\eta_{SSR} = \frac{1 - \left(\frac{f_b}{f_a}\right)^2}{(1 + \frac{f_b}{f_a})^2} \tag{2.58}$$

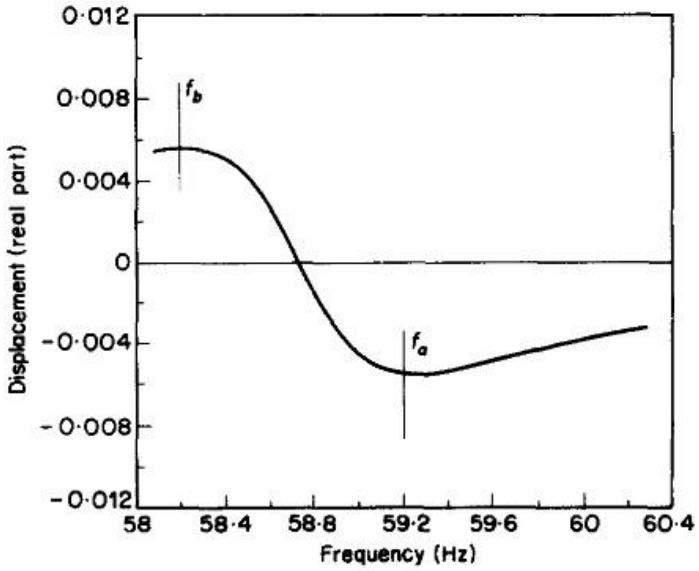

Figure 12 - Numerical prediction of the loss factor based on the real part of the response spectrum [40].

2.4 Half-power bandwidth method for modal data extraction

The half-power bandwidth method consists of determining the frequencies at which the amplitude of two consecutive points, A_1 and A_2 (see Figure 13), in the response curve of a dynamic system will equal $1/\sqrt{2}$ of the peak amplitude. This method has been successfully used for different types of material configurations in experimental testing. The modal loss factor can be determined by the ratio of the frequency interval between ω_1 and ω_2, $\Delta\omega = \omega_2 - \omega_1$, and the natural frequency value of each peak (equation (2.59)):

$$\eta = \frac{\Delta\omega}{\omega_n} \tag{2.59}$$

Where $\omega_1 = \omega_n(1-\xi)$ and $\omega_2 = \omega_n(1+\xi)$.

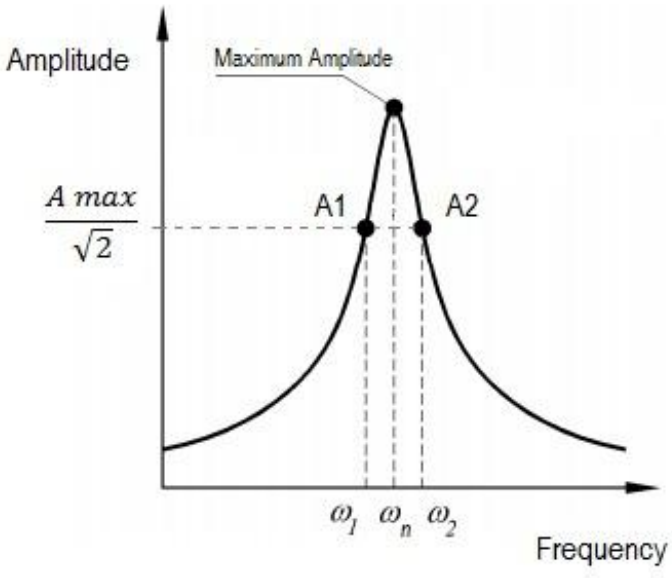

Figure 13 – Half-power bandwidth method.

2.5 Advantages of using CFRP and cork for aerospace applications

During this work, it was already mentioned some benefits of using composites with viscoelastic layers as a passive damping method. In the next paragraphs, the advantages of combining the viscoelastic properties of cork with a stiff CFRP laminate will be explored.

In an aircraft, the fuel consumption stands for a considerable part of the operating cost. Aeronautical engineers work in the development of new forms to create more efficient aero-engines, minimization of the aerodynamic drag, optimization of flight trajectories and more efficient light materials, aiming at reducing the operations fuel costs [41]. Therefore, the application of carbon fiber composite materials as structural components is growing rapidly due to the high specific stiffness and specific strengths combined with its great corrosion resistance, low volumetric density and maintenance cost [42].

Figure 14 illustrates the specific strength and stiffness comparison between different metals and alloys, quasi-isotropic glass fiber reinforced plastic (Glass/QI) and quasi-isotropic carbon fiber reinforced plastic (Carbon/QI), strengthening the idea of a general trend regarding

replacing metal by CFRPs. As an example, Figure 15 indicates the amount of composite materials used in the new Boeing 787.

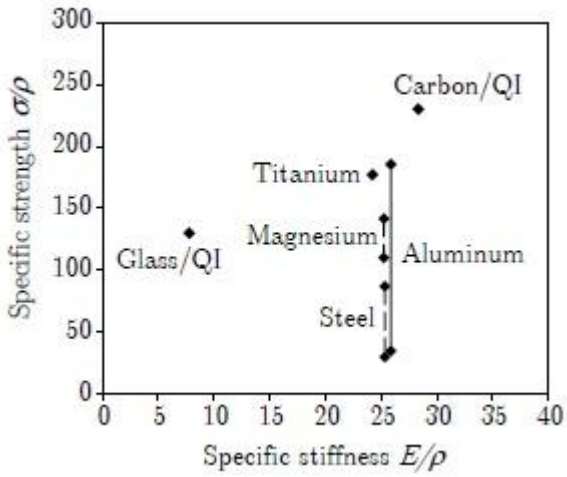

Figure 14 - Specific strength and stiffness comparison between different metals and alloys (quasi-isotropic glass fiber reinforced plastic (Glass/QI) and quasi-isotropic carbon fiber reinforced plastic (Carbon/QI)) [41].

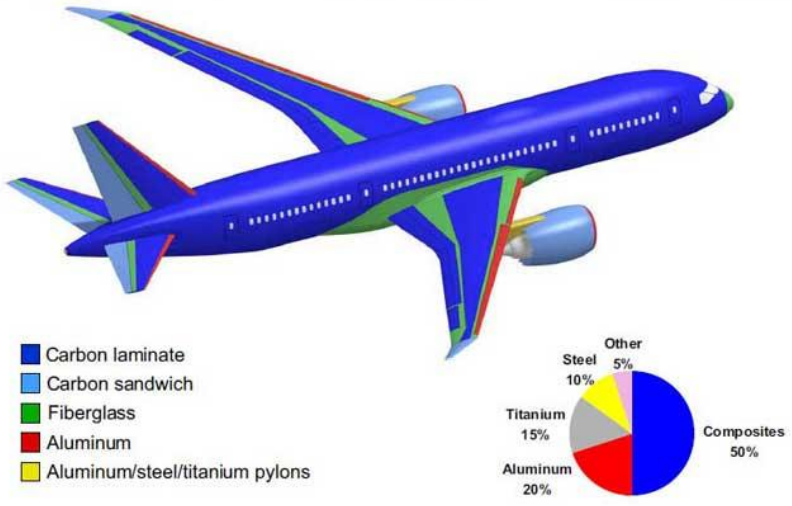

Figure 15 - Materials used in the new Boeing 787 (with a clear prevalence of CFRPs)

Regarding the viscoelastic material used in this work, the choice has been relying upon cork. Portugal and Spain are the world's main producers and exporters of cork based materials, and

a raising investment in research activities for engineering applications using this natural material has been booming over the last years. Cork is extracted from the outer layer of the cork tree, and its natural intrinsic properties are in the base of its great versatility in many types of applications, such as fishing boats, road pavements, floor tiles, garment ornaments, shoe soles and in stoppers for wine bottles, which is its most widespread use.

One remarkable propriety of this material is its low density due to the high gas content of the small structural cells (typically 40 μm average size). The high amount of gas entrapped in the closed cellular structure leads to excellent thermal insulating properties. Moreover, the low density and high porosity also provides great damping capabilities and low acoustic-vibration transmissibility.

When compared with other engineering materials, cork has lower stiffness. However, cork cells are strong and the specific strength of cork is as good as most rigid synthetic foams. Recently, the use of cork based materials has been investigated for different aerospace applications due its thermal properties, slow burn rate and shock absorption capacity [5] (see examples in Figure 16 and Figure 17). Silva et al. [43] analysed the damage tolerant properties of CFRP sandwich with cork-epoxy agglomerates as a core material through low velocity impact testing. Additionally, this work intended to evaluate the possibility of using such sandwich configuration combined with cork agglomerate as a form of improving the aeroelastic properties of aeronautical components. Results were conclusive about the superior energy absorption properties of cork based composites, which have an inferior extension of damage of both the core and facesheet materials when compared with polymethacrylimide foams.

Nevertheless, the life of aerospace structures and their inherent fatigue resistance optimization depends on a controlled vibration's amplitude that can be provide by sandwich components with cork agglomerates layers, which present an high energy absorption capacity with minimum damage probability, resulting in better crashworthiness limits during service [44]. Moreover, as a natural material, cork has considerable advantages in terms of sustainability and recyclability compared with other synthetic core materials. Therefore, it can become a suitable and effective material for innovative applications which require low cost, low density and high energy absorption.

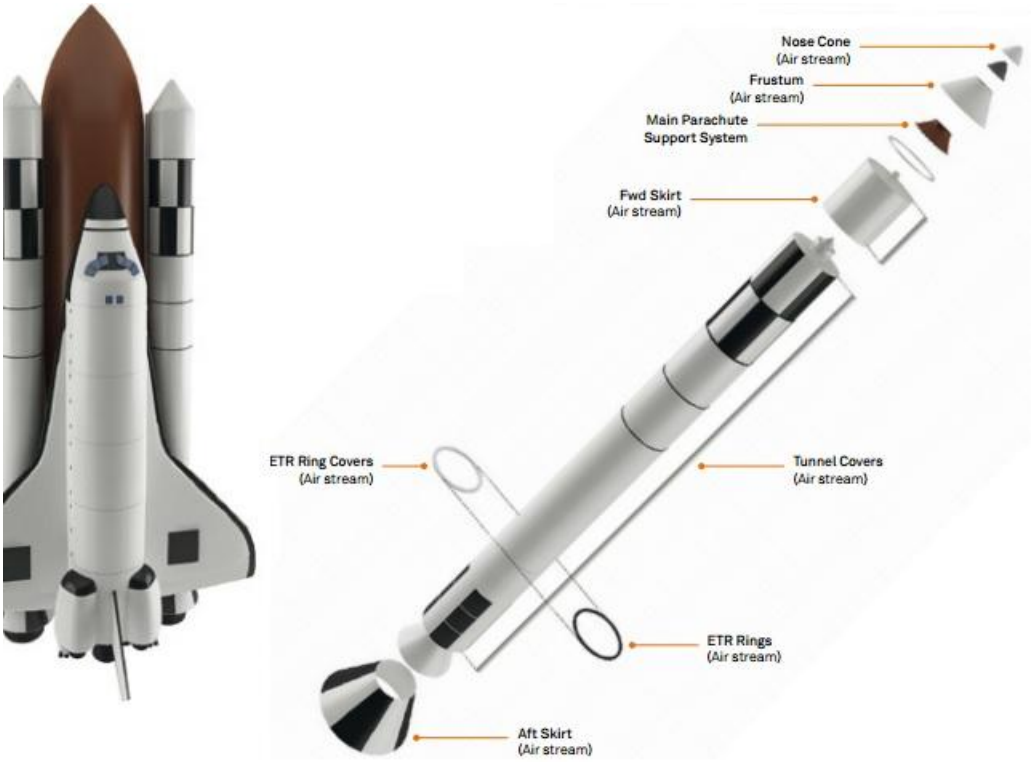

Figure 16 - Example of cork application in the propulsion system of Space Shuttle [45].

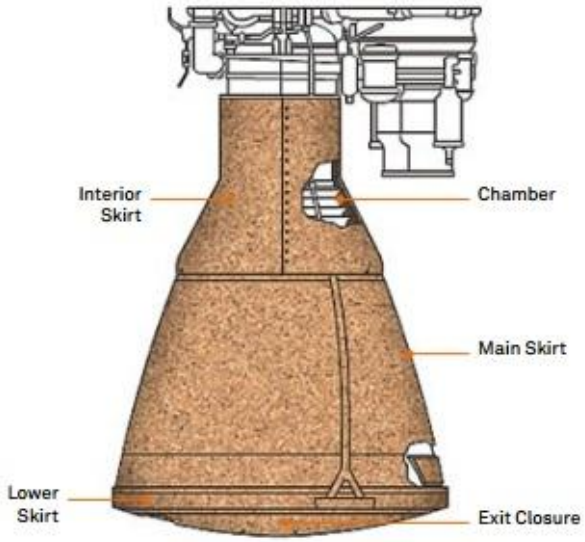

Figure 17 – Lightweight phenolic cork as a thermal protection material used in SCOUT Rockets [45].

Chapter 3

Numerical model

3.1 Introduction

Common structural systems exhibit fairly straightforward dynamic response in terms of numerical simulations. However, viscoelastic materials are slightly more difficult to model mathematically. Some of the biggest challenges in a viscoelastic materials' numerical model refers to the necessity of an accurate representation of the influence of different parameters, as seen in the previous chapter, such as temperature, frequency, cyclic strain amplitude, and environmental dependencies between the viscoelastic material properties and their associated effect on a structure dynamics [16].

The main objective of the numerical analysis implemented in this work is the dynamic response characterization of a rectangular flat plate representative of a sandwich component with a cork agglomerate core, which was attained using the commercial finite element method (FEM) code ABAQUS®. This code is widely used to analyse static deformations and for modal analysis, as it allows determining approximate solutions to boundary value problems, analysing the geometry by connecting many simple element equations over small subdomains and to approximate a more complex equation over a larger domain.[18, 46]. This has several benefits, like accurate representation of complex geometry, capacity to handle a wide variety of engineering problems, inclusion of dissimilar material properties, ability to represent complex loadings and to analyse local effects [26, 47].

In the present case, CFRP laminates were modelled based in a composite shell and the dissipative effect of the viscoelastic layer is evaluated having the behaviour of a plain CFRP (i.e., without cork) as a baseline material. For the analysis of modal loss factor, a free boundary condition was applied to the plate (Figure 18a), since this is representative of the experimental conditions described in the following section. On the other hand, and to study the harmonic response of the plate and the influence of cork on damping, a second case was considered fixed at one end (Figure 18b). In both cases, the plate was subjected to an impulsive concentrated 1N load applied at the centre of the free tip. The impulsive force simulates an hypothetic operational condition of the system represented here by the impact of the hammer. Ideally, if the impulse time is small, it causes a constant amplitude vibration over the frequency domain and all modes of vibration of the structure will be excited. Impact hammers are suitable for smaller, lightweight structures where the signal-to-noise ratio is

better for taking measurements. Moreover, the small force value was selected to avoid large displacements and to maintain the validity of linear theory.

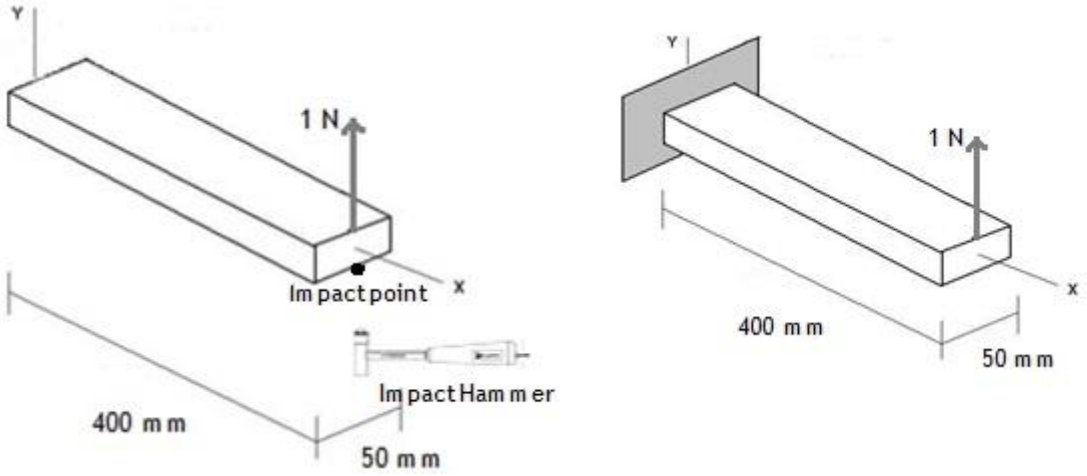

(a) Free-to-free boundary condition with impulsive load.

(b) Fixed end boundary condition with impulsive load.

Figure 18 – Illustration of the boundaries conditions and applied load as considered in the numerical model.

A field output was created to extract the displacement of the beam for further evaluation in frequency domain and to characterize the influence of using cork as embedded viscoelastic material in the dynamic response. Hence, it is fundamental that the model of the beam system can be able to accurately represent the strain energy due to the shearing effects in the core material, since this mechanism is considered the dominant source of damping followed by the dissipative effects arising from the interactions between fibres and matrix of the composite material. Such analyses lead to a development of a general viscoelastic numerical model. Hence, numerical results were validated from a direct comparison with experimental data obtained for identical conditions, which allows an extrapolation of the adopted modelling procedures to other cases (depending on the abovementioned test variables).

3.2 Material and configuration

Most of the computational methods predict viscoelastic damping characteristics based in preconceived damping ratios or other damping parameters estimated by experimental results.

Modelling viscoelastic behaviour in ABAQUS® requires some input parameters, as the mass proportional damping factor (α) and the stiffness proportional damping factor (ß) defined in chapter 2. Hence, for the numerical model, these values will be estimated using equations (2.47) and (2.49) from section (2.2.5). The respective modal damping factor, which is half of the modal loss factor, is given by experimental results. Such experimental calculations involve the fraction of critical damping for the first mode of resonant vibration, which may be defined as in equation (3.1), being ψ the specific damping capacity value. This equation is valid for vibrating systems having a value of ψ < 100.

$$\psi = \frac{\xi}{4\pi} \tag{3.1}$$

Hence, α has an important influence in the numerical results. Since this parameter is dominant for low frequencies, α values are averaged for the first two vibration modes for each laminate's configuration type. As expected, the values obtained for ß were very low, or even zero, for all specimens. Moreover, the complex Poisson's ratio plays an important role in characterizing the linear dynamic behaviour of solid materials. The ratio of the imaginary part to the real part of complex Poisson's ratio is referred to as Poisson's loss factor and its magnitude does not exceed 0.1 even if shear damping is high. Nonetheless, typical Poisson's loss factor based on a high loss rubbery material may be lesser than 0.1 [48]. Besides, the Poisson's ratio of Cork is close to zero showing very little lateral expansion when compressed [5]. Herewith, for a given finite element model with certain mass and stiffness matrices, it is quite clear that the results of the dynamic analysis depend hugely on the numerical assignment of those parameters, corroborating the importance of the validation of results through experimental data.

As a consequence of the anisotropy of cork viscoelastic properties, the storage modulus is higher towards the transverse prismatic direction. For the other directions, the properties can be considered almost uniform. Thus, as in other numerical works, the cork based sandwich has been modelled considering isotropic conditions [49].

There is also a possible resin transferring from the facesheets to the cork core during the curing cycle. The existence of resin inside the cork layer means a rigidity increase and therefore a higher Young's modulus. This type of uncertainty has to be taken in consideration when analysing possible deviations in the numerical results.

In the particular case of the cork agglomerates used in this thesis, the main mechanical properties were provided by the material's manufacturer, Amorim Cork Composites (Portugal), which were obtained by a dynamic mechanical thermal analysis technique (DTMA).

A total number of 11 batches were considered, divided in plain CFRP laminates (i.e., without viscoelastic layer) and CFRP + viscoelastic layer. Table 4 shows all the 11 batches considered according to the intended testing variables, namely, lay-up staking sequence, inclusion of viscoelastic layer and its relative position within the laminate. The viscoelastic layer consisted of a 1mm thick NL 10® cork agglomerate. The main mechanical properties of the cork agglomerate material can be found in Table 5, whereas the characteristics of the CFRP laminate are summarized in Table 6.

Table 4 - CFRP laminates staking sequences

Type	Stacking sequence
A1	$[\,0\,]_{3S}$
A2	$[0_3$ / C / $0_3]$
B1	$[0/\,90\,/0]_S$
B2	[0/90/0/ C /0/90/0]
C1	$[\,0\,]_{6S}$
C2	$[0_6$ / C / $0_6]$

Type	Stacking sequence
D1	$[0/\,90]_{3S}$
D2	[(0/90) $_3$ / C / (90/0) $_3$]
E1	$[0_2$ / C / $0_4]$
F1	$[0_3$ / C_2 / $0_3]$
G1	$[0_2$ / C / 0_2/ C / $0_2]$

Table 5 – Mechanical properties of the cork agglomerate core

Density	120 [kg/m3]
Poisson's ratio	0.1
Tensile strength	0.6 [MPa]
Shear modulus	5.9 [MPa]
Loss factor (at 1kHz)	0.022

Table 6 – Mechanical properties of CFRP laminate

Density	1500 [kg/m3]
Poisson's ratio	0.25
Longitudinal Young's Modulus	170 [GPa]
Transversal Young's Modulus	6.7 [Gpa]
Shear modulus	5 [GPa]

3.2.1 – Laminate preparation and experimental set-up

The experimental part of this work consisted in the fabrication of 33 specimens made of a high strength unidirectional carbon-epoxy laminate using a hand layup process. Specimens with dimension 400 x 50 mm were cut from a carbon-fibre unidirectional roll tape with a 215 g/m^2 mass fraction. To account for final trimming process, the cut dimensions had a 3 mm exterior margin. Prior to the hand layup process, an acrylic glass mould surface was prepared, cleaned and dried. Then, a mould release agent was applied, in circular movements, using a small piece of cloth following the respective time and applications instructions. For the lay-up process, an epoxy resin system (SR1500 and respective SD2503 hardener) was used at room temperature according to the manufacturer's datasheet. After curing, all specimens were submitted to a final finishing process using sand-paper and a cutting disk to obtain the required nominal dimension. Figure 19 shows some photos of the fabrication process, whereas Figure 21 refers to some images of the cork based agglomerate used in this work.

(a) Unidirectional carbon fiber roll-tape.

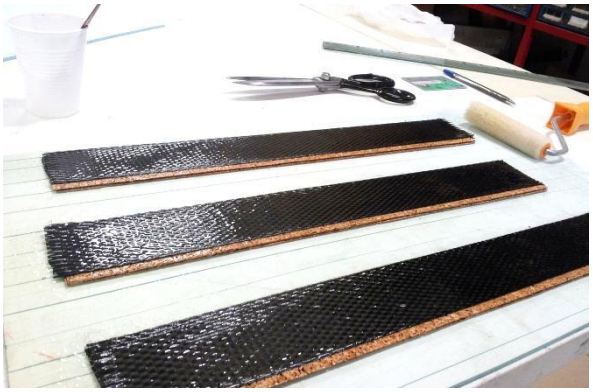

(b) Three specimens with embedded cork layer made from a hand lay-up process.

(c) Final look of a CFRP specimen.

(d) Cross section detail of a G1 type specimen.

Figure 19 – Photos of the laminates' preparation and some final details.

As mentioned before, specimens were analysed using the half-power bandwidth method, following the general procedures indicated in ASTM E756 (1998) [50], aiming at characterizing

the loss factor for each sample. These tests were made in the Vibrations and Experimental Analysis Laboratory of EST/IPS (Setúbal, Portugal).

An illustration of the testing apparatus is shown in Figure 20. Specimens were placed free in space (suspended by two nylon threads on a rigid frame) and excited with a Dyna Pulse (Dytran Instruments) instrumented impact hammer. The frequency response was obtained by indirect measure with a Brüel&Kjær 4374 accelerometer, located on the lengthwise direction at the opposite side of the hammer impact point. The hammer impact characteristic was obtained from a sensor placed on the hitting face.

A total of four tests were made for each type of specimens and a series of ten shots was performed in each specimen which were acquired by the transducer considering a valid shot whenever the coherence value was close to unity. The data were processed on a computer using two software programs: Vibpro® and LabView®. The first code is used for pre-processing purposes in conjunction with a spectrum analyser and a signal conditioner to obtain the representation of the frequency response. The latter code is used to determine the resonant frequencies and the loss factor using an in-house routine consisting of an algorithm that automatically extracts points 3dB below each peak.

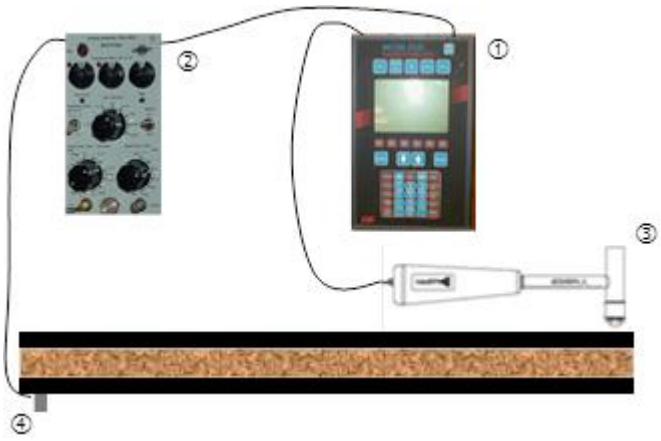

Figure 20- Schematic representation of the experimental installation.

① - Spectrun analyser CSI 2120

② - Conditioner and Amplifier Brüel&Kjær 2635

③ - Instrumented hammer Dytran Instruments, DYNA PULSE

④ - Acelerometer Brüel&Kjær 4374 with 0.65g mass (excluding cable)

(a) Roll of CoreCork® NL10 used in this work.

(b) Used cork detail.

Figure 21 - CoreCork® NL10 used for the experimental set.

3.3 Mesh

The discretization of the structure domain into sub-elements allows to create a mesh, which is dependent on geometry, material properties, load and boundary's conditions. In this work the geometry of the plate is quite simple providing an easy mesh application. Like similar works with plane shell parts, a structured type mesh was used. In this case, each node is defined by a position (x; y; z) referred to Cartesian axis in the general domain. The elements were applied to the model by a sweep generated mesh technique composed of several *quadrilateral-dominated* S4 elements. These are general-purpose shell elements which are widely used in numerical simulations due to their suitability for both thin and thick shell problems. Regarding these specifications, a mesh quality performance evaluation was performed using a convergence analysis of the natural frequencies as the targeting output in order to settle a compromise between computing time and results accuracy aiming at obtaining an adequate mesh refinement. The convergence analysis lead to a structured mesh with a total of 3600 shell type element and 3819 nodes, as shown in Figure 22. A detailed image of the final mesh is illustrated in Figure 23.

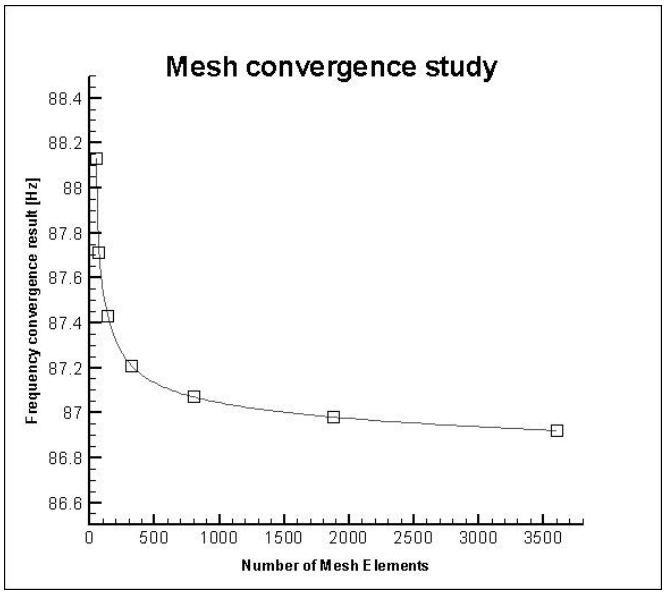

Figure 22 – Mesh convergence study for the first resonant frequency (A1 sample).

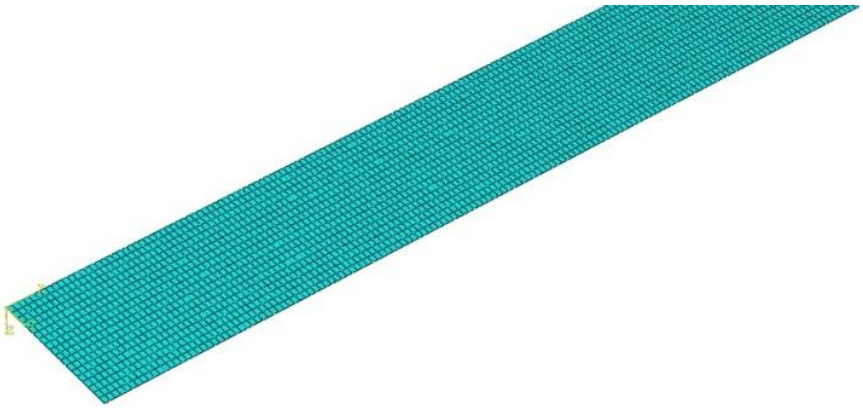

Figure 23 – Detail of the final mesh after the convergence study.

3.4 Model validation

To confirm that the numerical model is capable of providing a realistic response representative of a CFRP sandwich with a constrained cork layer, results were compared with experimental data obtained in similar conditions. The plate was simulated with free-to-free boundary conditions with an instantaneous concentrated force (1N amplitude) applied at the

centre of the plate tip. Thus, the damping characteristics were evaluated by comparison between the obtained numerical and experimental loss factors.

Figure 24 presents the experimental and numerical results in order to verify the model precision for two representative cases: a) a $[0]_{3S}$ unidirectional CFRP laminate without viscoelastic layer; b) a $[(0/90)_3$ / C / $(0/90)_3]$ cross-plied CFRP laminate with an embedded viscoelastic layer.

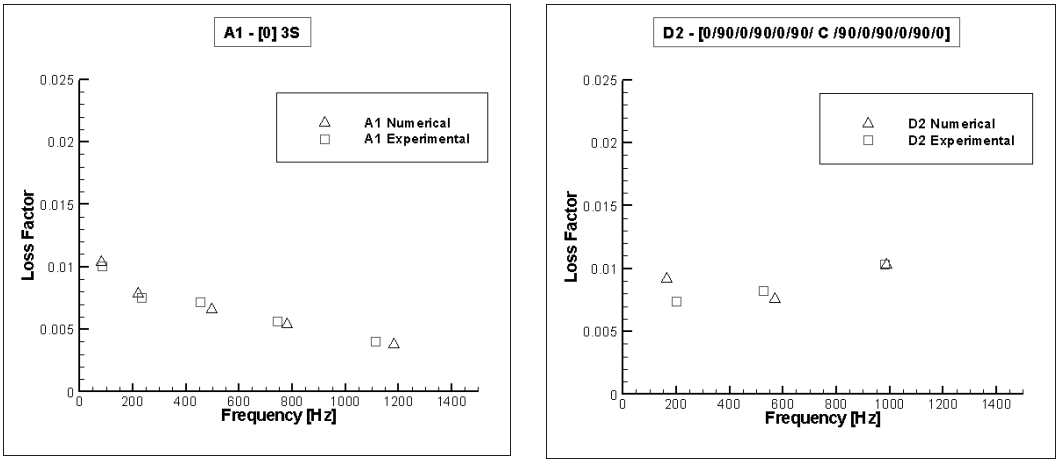

(a) (b)

Figure 24 - Comparison between numerical and experimental data considering two different specimens types: a) unidirectional CFRP without viscoelastic layer; b) cross-plied CFRP with embedded viscoelastic layer.

As it can be seen, there is a good correlation between numerical and experimental data whichever the case. This matching in the results has been also observed for all others specimens' configurations, which allowed determining an average deviation of 7.9% on the loss factor value, which is less than typical experimental scatter. Similar results for the other specimens studied in this thesis can be found in Annex A.

As far as the numerical loss factor determination is concerned, it was related with each resonant peak and the respective mass proportional damping factor (α) value. Since α is dominant at low frequency ranges, which are of particular interest in this study, the results dependency on the mass proportional damping effect becomes obvious. Thus, and to ensure a greater accuracy of results, the component's natural frequencies extracted in the numerical simulations were related to the corresponding mass proportional damping factor values according to the following expression:

$$\eta_{i,num} = \frac{\alpha_i}{\omega_n} = \frac{2\,\xi_{i,exp}}{\omega_{n,num}} \tag{3.2}$$

In equation (3.2), $\xi_{i,exp}$ is the damping ratio acquired in the experimental set and $\omega_{n,num}$ is the natural frequency estimated in the numerical analysis. The results in the following section summarize the experimental and numerical analyses for each specimen tested regarding the effects of design parameters on loss factor.

Chapter 4

Results

4.1 Effects of design parameters on loss factor

Numerical model offers the possibility to estimate the loss factor of composite laminates depending on the effect of several design parameters, providing a better understanding and characterization of the embedded viscoelastic layer effect on damping for each resonant frequency. The following sections summarizes these effects on damping results having a plain CFRP specimen as baseline material. In all cases, simulations follow identical conditions to the ones adopted during experimental testing.

4.1.1 Effect of ply orientation angle

Figure 25a shows the behaviour of two material's samples (A1 and B1) with different stacking sequences. Note that in either cases there is not any viscoelastic layer embedded in the laminate since it is intended to assess the solely effect of the ply orientation angle in the damping characteristics of the material. As it can be seen, the loss factor variation as a function of frequency is identical in both cases, but presenting higher values for the cross-ply laminate towards the upper limits of the frequency range. Also, a slight decrease of the modal resonance frequencies is noted for the 90 degrees ply orientation (specimen B1).

Figure 25b presents the comparison between samples A2 and B2, both with a viscoelastic layer. Again, the trend in the loss factor variation is identical but now the unidirectional laminate presents marginally higher values, particularly for frequencies above 800 Hz. Alongside with the damping increase resulting from the use of the viscoelastic material, a reduction in the modal natural frequencies regarding the use of 90 degrees ply orientation (specimen B2) is also observed.

The effect of the laminate thickness was also evaluated by extending the numerical analysis to specimens with twice the number of layers but maintaining the same layup stacking sequence. Figure 26a refers to unidirectional and cross-ply specimens with 12 layers but without the inclusion of cork (specimens C1 and D1, respectively). As it happens with samples without viscoelastic layer, there is a low damping effect as a consequence of the ply orientation change. In this case, it seems that the effect of angle orientation is lessened by

the mass and stiffness increase as a result of the higher number of laminate's plies. However, the inclusion of a viscoelastic layer causes a notable change in the loss factor values for the whole frequency test range, compared to the thinner specimens, which is particularly significant for the unidirectional type laminates (specimens C2), as visible in Figure 26b.

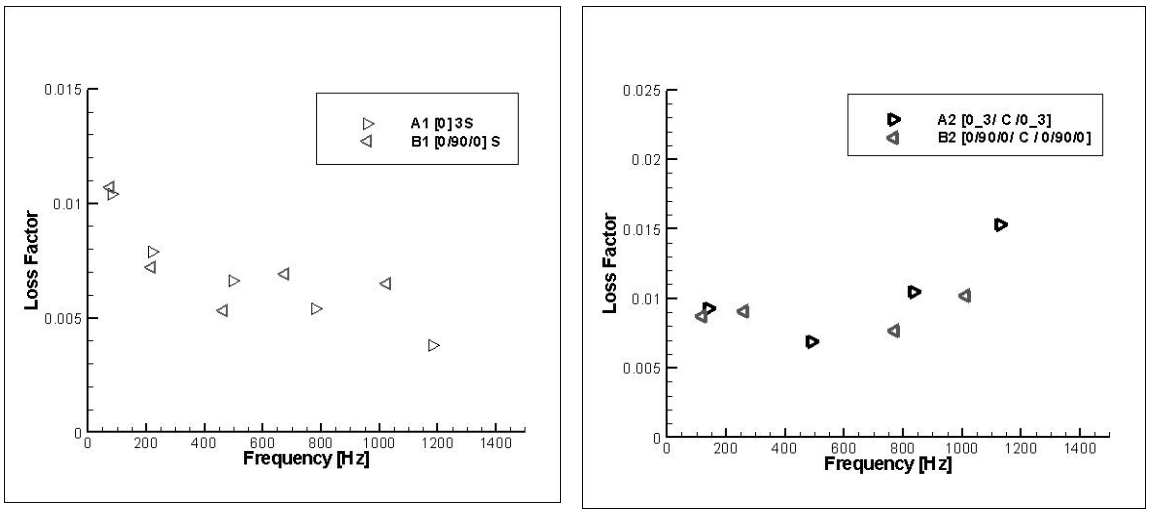

(a) (b)

Figure 25 – Loss factor variation as a function of layup stacking orientation: a) unidirectional (A1) and cross-ply (B1) specimens without viscoelastic layer; b) unidirectional (A2) and cross-ply (B2) specimens with viscoelastic layer in the middle-plane.

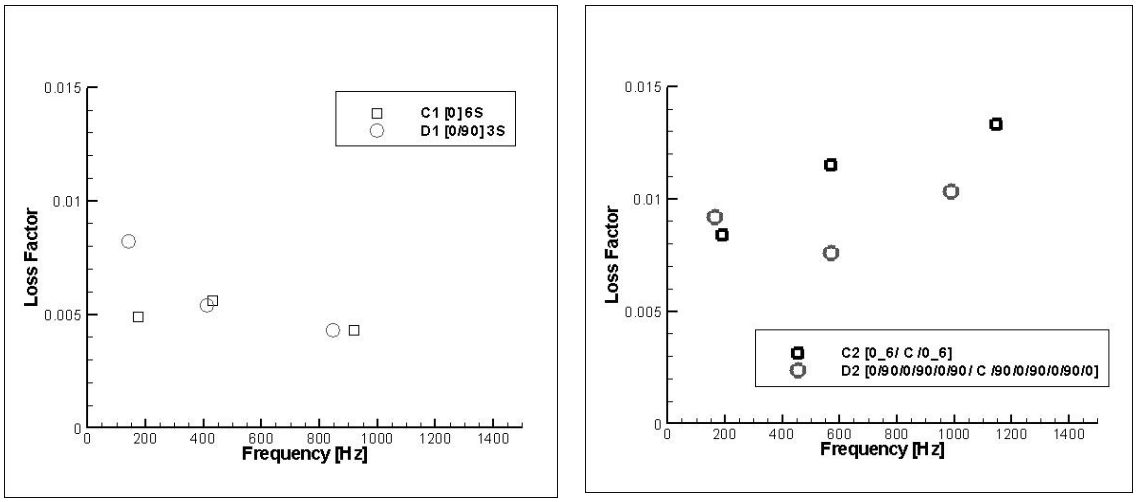

(a) (b)

Figure 26 – Loss factor variation as a function of layup stacking orientation for thicker laminates: a) unidirectional (C1) and cross-ply (D1) specimens with 12 layers without cork; b) unidirectional (C2) and cross-ply (D2) specimens with 12 layers and considering a cork-based layer in the middle-plane.

4.1.2 Effect of laminate's thickness

The laminate's thickness effect was assessed by determining the loss factor variation for specimens having the same layup stacking sequence but with a distinct number of composite layers, namely 6 or 12 layers. Whichever the case, a cork based layer was always considered in the laminate's middle plane as it was demonstrated before that the utilization of this viscoelastic material favours the damping characteristics of the host material.

Figure 27a compares the thickness effect in cross-ply specimens, whereas Figure 27b refers to unidirectional type specimens. It can be seen that the thickness effect is nearly negligible in both cases though the unidirectional specimens shows higher average loss factor values (especially for frequencies above 400 Hz).

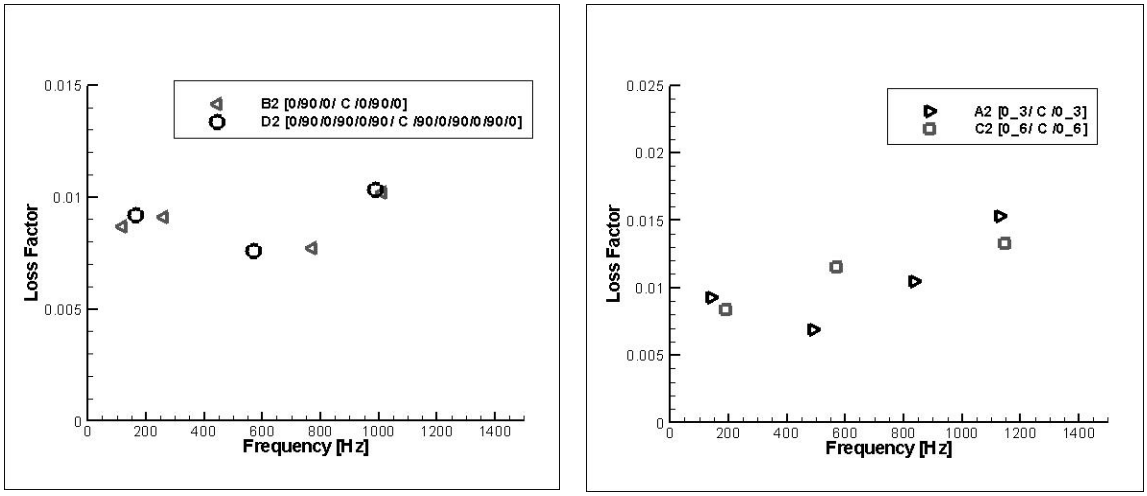

(a) (b)

Figure 27 – Loss factor variation as a function of the laminate's thickness: a) cross-ply specimens; b) unidirectional specimens.

4.1.3 Effect of the viscoelastic layer relative thickness

Considering the same laminate's number of layers and ply angle orientation but with the twice of viscoelastic material thickness placed in the same position (i.e., middle-plane), Figure 28 demonstrates, as expected, an increase of the loss factor as a result of the addition of a higher amount of viscoelastic material. The loss factor variation with frequency is nearly linear and the modal natural frequencies are slightly shifted mainly because of the greater mass and damping contribution of the extra thickness of the cork-based layer.

A MATLAB® program using the Ross-Kerwin-Ungar damping model [35] described in section 2.3.1 was developed to obtain an estimation of the loss factor variation as a function of the thickness of the cork layer. This procedure allowed determining the viscoelastic behaviour for the first three vibration modes of an A2 type laminate, i.e., with a $[0_3/C/0_3]$ stacking arrangement.

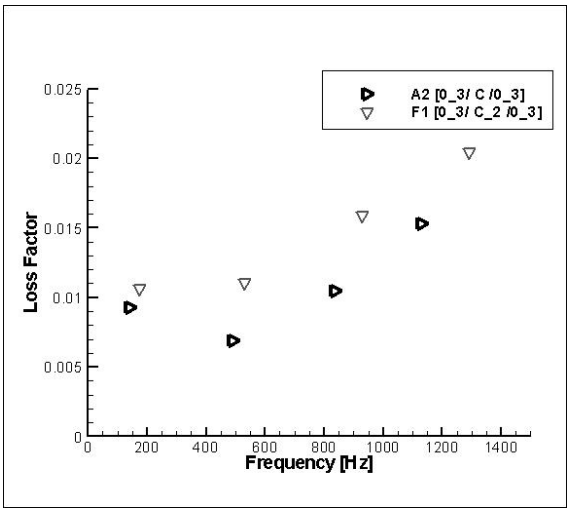

Figure 28 – Loss factor variation as a function of the viscoelastic layer thickness.

Figures 29, 30 and 31 present the analytical plots against numerical results considering the first three vibration mode. It is clear that there is a good correlation between the two approaches, which is visible by the identical variation trend of loss factor with frequency and discrete results for higher frequencies. As a general conclusion, it can be said that the damping capabilities of the material follows directly the thickness of the viscoelastic layer up to a 4-5 mm threshold, although with different slope rates. However, the increase of the damping effect seems to diminish as the viscoelastic layer thickness increases, which is noticeable by the plateau in both analytical and numerical results for high thicknesses values. In fact, the loss factor predicted for the third mode converges more quickly as the viscoelastic layer thickness increases, enabling to choose the best design option for each modal frequency range. This is an important conclusion as it means that the damping capabilities of a composite material do not necessarily follow a direct relation (in terms of the loss factor variation) with the thickness increase of the viscoelastic layer (having the same laminate thickness as baseline). Actually, the gain in the loss factor due to the addition of viscoelastic material may not compensate for the weight increase affecting the overall component, which is a critical requirement in certain types of applications (such as aeronautic structures).

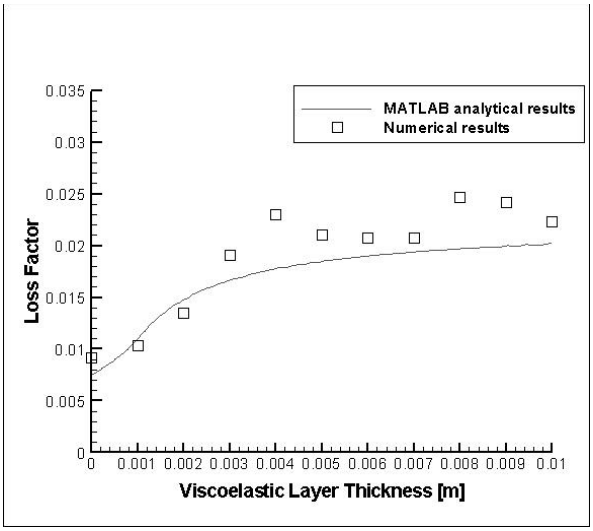

Figure 29 - Analytical vs numerical results regarding the loss factor variation with viscoelastic layer thickness for the first vibration mode.

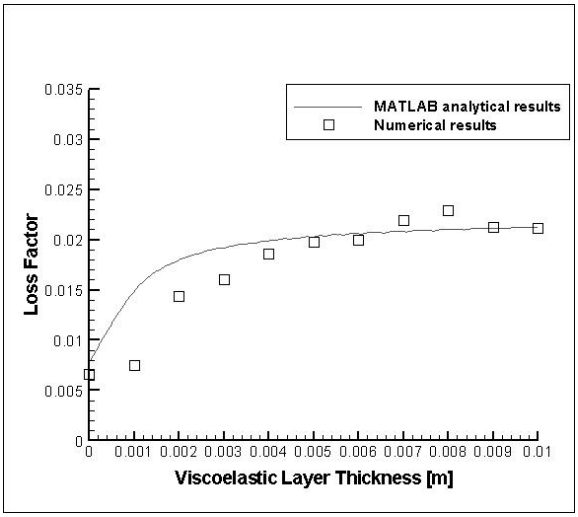

Figure 30 - Analytical vs numerical results regarding the loss factor variation with viscoelastic layer thickness for the second vibration mode.

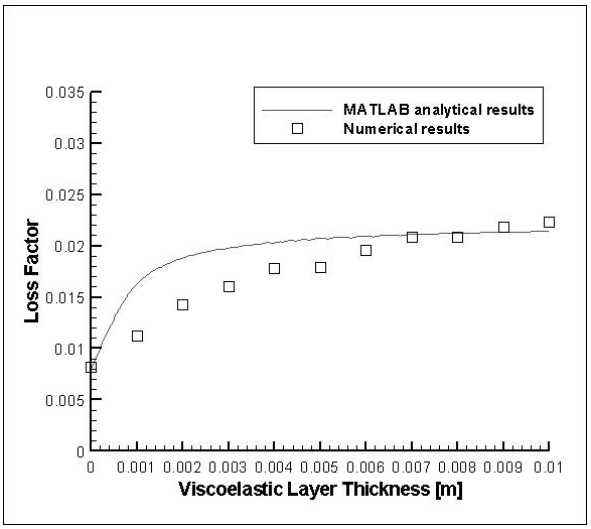

Figure 31- Analytical vs numerical results regarding the loss factor variation with viscoelastic layer thickness for the third vibration mode.

4.1.4 Effect of the viscoelastic layer relative position

The relative position of the viscoelastic layer along the thickness wise direction of the laminate is another important parameter with a likely effect in the loss factor value. Having this in mind, two different specimen configurations were considered for numerical analysis having the cork-based layer in two distinct positions: in the laminate's plane of symmetry (specimen A2); towards the laminate´s outer surface (specimen E1). Figure 32 shows the loss factor variation for these two cases considering a unidirectional type specimen with 6 layers. These results show that there is a slight effect of the viscoelastic layer position regarding the damping characteristics of the material. This can be explained by the small relative distance between the two cases herein considered which, in part, has been constrained by the limited laminate's thickness and consequent difficulties of reproducing experimental specimens with an embedded cork layer positioned near the surface.

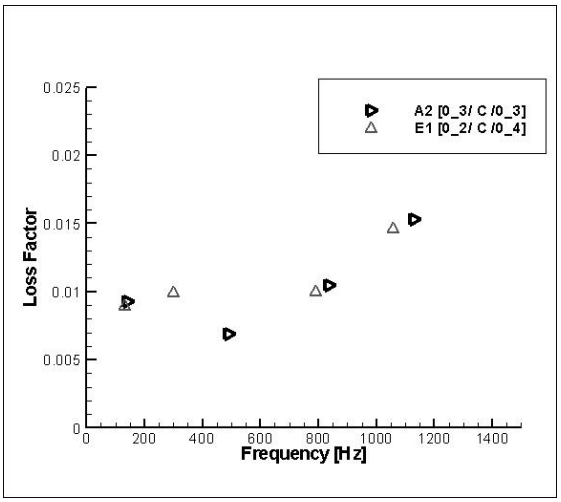

Figure 32 - Loss factor variation as a function of the viscoelastic layer's relative position (single layer case)

To overcome this issue, another approach has been followed consisting in the simulation of the damping behaviour of an identical laminate but with two viscoelastic layers. This allows to strengthen the energy loss contribution of the damping material (as it is now two times thicker than the previous case) and therefore try to perceive any effect resulting from the variation of the position of the viscoelastic layer. A similar approach has been adopted by Zhang et al. [51] who successfully demonstrated that there is an optimum thicknesswise location for the viscoelastic layer in order to obtain a maximum loss factor value.

The plots in Figure 33 refer to unidirectional type specimens also having the cork-based material (now in the form of two layers instead of the single one considered in the previous case) in two distinct positions: in the laminate's plane of symmetry (specimen F1); towards the laminate´s outer surface (specimen G1). Now, the effect of the relative position of the viscoelastic layers in the loss factor variation is quite clear, as the middle-plane case provides higher damping capabilities than the one with the cork-based layer shifted towards the specimen's outer surface. This effect is particularly perceptible in the upper limit of the testing frequency range, where the loss factor value is around 20% higher than that for specimens with two viscoelastic layers offset from this position.

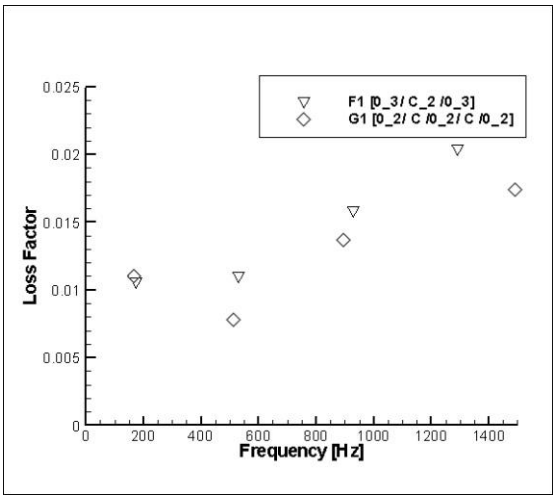

Figure 33 - Loss factor variation as a function of the viscoelastic layer's relative position (double layer case)

4.2 Vibration response

A secondary goal of the numerical simulations was to determine the magnitude (displacement) response of each type of specimen's configuration in the frequency domain. For the sake of demonstration purposes, results regarding specimens A1 and A2 (unidirectional type) are presented in Figure 34. . The plots concerning the remaining laminate's types can be found in Annex B. As expected, the displacement peaks are obtained in the vicinity of resonant frequencies and the damping effect due to the embedded cork layer is reflected by the reduced displacement field of specimen A2. Moreover, the viscoelastic properties of cork cause a shifting effect of the resonant frequencies when compared to the plain CFRP A1 specimen. This type of information is important to support the design criteria of certain types of structures which may be subjected to detrimental effects (fatigue, fretting, etc.) caused by dynamic loading conditions.

From the Figure it is also clear that the inclusion of cork increases the natural frequency values and decreases the respective peak amplitude. Additionally, and despite the prevalence of bending modes, some peaks corresponding to torsional modes and residual frequencies are possible to observe, especially near high displacements. Such residual modes can be explained because the ABAQUS®output source is a direct consequence of the point of force

application. Figure 35 presents the first four mode shapes obtained from the numerical model for a A2 type laminate (with cork, left fixed end).

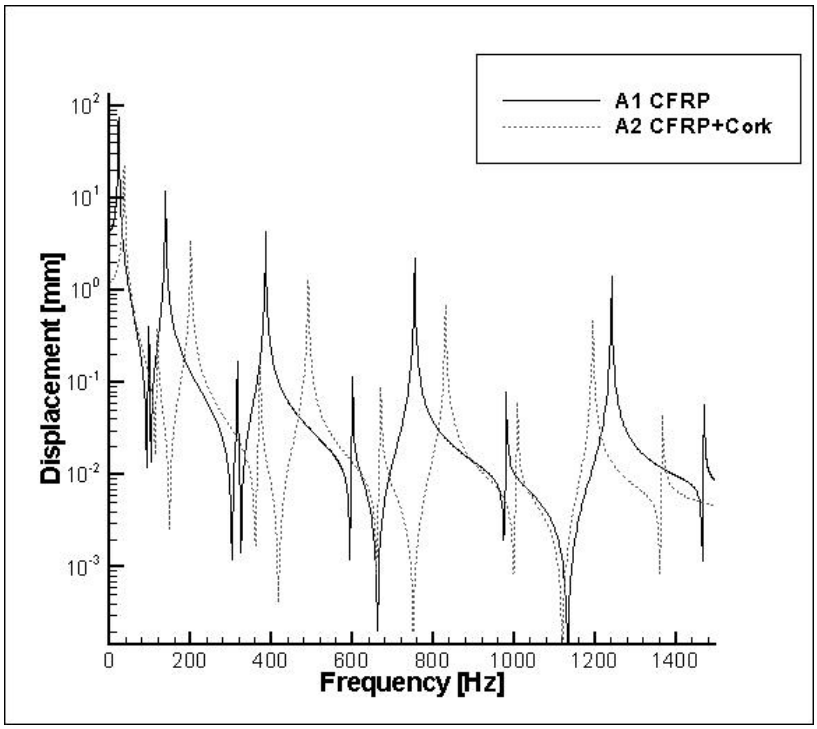

Figure 34 – Dynamic response in frequency domain of specimens A1 and A2.

(a) 1st mode shape

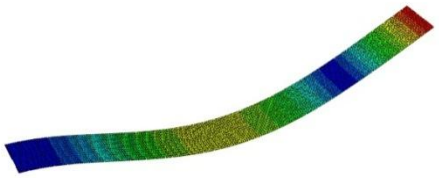

(b) 2nd mode shape

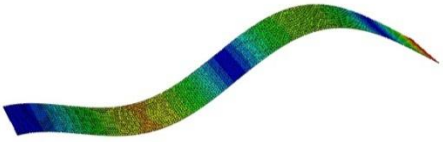

(c)3rd mode shape

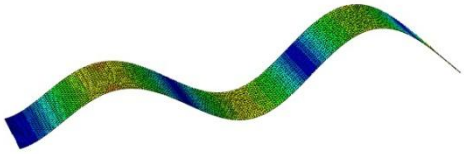

(d)4th mode shape

Figure 35 - Mode shapes obtained from the numerical model for a CFRP + Cork (A2 type with left fixed end).

4.3 Summary of results

Given the various effects of design parameters on the loss factor variation, we are now in position to point out the best material's configuration for the maximization of the damping characteristics. This information is determinant to support a judicious design phase of composite laminates with embedded viscoelastic layers.

Table 7 is a summary of numerical results regarding the best laminate configurations for each vibration mode. The percentage variation are calculated having the plain CFRP sample as reference and considering and identical number of reinforcing plies. As far as damping is concerned, configuration G1 ([0_2/ C /0_2/ C /0_2]) is the best solution for the first mode of vibration, presenting a 6% increase in the loss factor. For the second mode, the increase on damping ascends up to 129% for the C2 type configuration ([0_6 / C / 0_6]), which in fact is the one with greater loss factor. The increase tendency on the loss factor is particularly notable for high frequencies, as the variation for the third mode is 198% and 276% for the last mode analysed. In both cases, the best material configuration is specimen F1, which corresponds to a material's configuration with a double-cork layer in the laminate's middle plane.

Table 7 – Best CFRP type configuration for optimum modal loss factor

Mode of vibration	***Maximum* loss factor (η_{num})**	**Configuration Type**	**Percentage variation** (compared with the plain sample)
Mode 1	0.0110	G1 [0_2 / C / 0_2/ C / 0_2]	6 %
Mode 2	0.0125	C2 [0_6 / C / 0_6]	129 %
Mode 3	0.0159	F1 [0_3 / C_2 / 0_3]	198 %
Mode 4	0.0204	F1 [0_3 / C_2 / 0_3]	276 %

Chapter 5

Conclusions

This study characterizes the effects and dynamic response resulting from the application of a constrained viscoelastic layer in CFRP laminates as a passive damping treatment. Numerical results, supported by experimental data, are quite conclusive about the improvement of damping characteristics as a result of the inclusion of a viscoelastic cork based material. The effect of the distinct design variables was evaluated through a parametric study which allowed to draw the following major conclusions:

- The introduction of a viscoelastic layer proved to be an effective solution to improve structural damping without implying a significant increase in the system's structural weight. In general terms, loss factor values for hybrid cork-based composites revelled to be twice of those for plain composites (average numbers and for the same layup stacking sequence);

- The damping effects become predominant towards the upper limit of the frequency range considered in this work (from 10 to 1500 Hz);

- Layup stacking sequence has a distinct influence on the damping properties of laminates depending on the presence of a viscoelastic layer. In fact, while plain CFRP specimens showed an undistinguished effect regarding the fibre arrangement, unidirectional cork-based materials presented a higher loss factor value against cross-ply laminates. Furthermore, this effect becomes more evident for higher laminate thicknesses, indicating that the layup sequence can be a very important design variable in thicker composites;

- The thickness of the viscoelastic layer has a strong influence in the loss factor value, showing a nearly linear dependency up to 4-5 mm. Beyond this threshold, the loss factor variation is much smaller and tends to a stable value, which means that the gain in damping capabilities can be compromised by the considerable weight increase of the laminate. Such conclusion is of a particular interest for aerospace applications regarding the systems' weight saving;

- Specimens with the viscoelastic layer placed in the laminate's middle-plane provide higher loss factor values than other relative positions along the thickness wise

direction, which can be explained by the dissipative effect resulting from high shear loading between the damping layer and constraining layers;

- From the loss factor percentage variation observed between specimens with and without cork layer, it is possible to conclude that the damping effect resulting from the viscoelastic material is more substantial for high frequencies. In fact, for the first mode of vibration the percentage variation is only around 6%, whereas in the fourth mode loss factor increases more than twice;

- The model validation provides useful information concerning the results' accuracy and validity. The average percentage difference between experimental and numerical results was inferior to 7.9%, which is less than typical experimental scatter. Such numerical model may be presented as a great study platform capable to provide easier, cheaper and faster damping characteristics estimation (especially of composites with constrained viscoelastic layers) when compared with experimental methods.

These conclusions are unquestionable about the feasibility of using composite materials with viscoelastic materials in many engineering applications where vibration control is required, without compromising (in a significant scale) the system weight. However, such widespread solution will constantly entail viscoelastic numerical models concerning the respective dynamic behaviour of the overall structure. Consequently, engineers have to persistently continuing the development of more accurate models, with less limitations, to characterize the impact of vibrations on the integrity of aircraft structures.

Future work

Despite of the good correlation between numerical and experimental results, there are some viscoelastic theories needing to be implemented to improve the model accuracy and to validate its applicability for others types of viscoelastic materials. Furthermore, an optimization procedure could be developed to provide additional information about important design aspects for this type of materials, allowing a more precise and throughout full knowledge about damping optimization.

References

[1] M.J.L van Tooren, G. La Rocca, L. Krakers, and A. Beukers, “Design and technology in aerospace. Parametric modeling of complex structure systems including active components,” *13th International Conference on Composite Materials*, 2003.

[2] J. Pora, “Composite Materials in the Airbus A380 - From History to Future”, *Proceedings ICCM-13*, 2001.

[3] S. Vasudeva, R. K. Kapania, E. M. Cliff, and P. Tarazaga, “Estimation of Elastic and Damping Characteristics of Viscoelastically Constrained Carbon Strands”, *Structural Dynamics and Materials Conference (SDM)*, 2006.

[4] M. Píriz , "*Passive vibration control of aerospace structures based on viscoelastic materials*", Covilhã: Universidade da Beira Interior, 2011

[5] S. P. Silva, M. a. Sabino, E. M. Fernandes, V. M. Correlo, L. F. Boesel, and R. L. Reis, “Cork: properties, capabilities and applications”, *International Materials Reviews*, vol. 50, Dec. 2005.

[6] J.M. Silva, M. Píriz, P.V. Gamboa, R. Cláudio, N. Nunes, J. Lopes, "A passive approach to the development of high performance composite laminates with improved damping properties", *The Eleventh Intern. Conf. on Computational Structures*, 2012.

[7] L. Gil, “Cork Composites: A Review”, *Materials*, vol. 2, no. 3, pp. 776–789, 2009.

[8] K. L. Napolitano, W. Grippo, J. B. Kosmatkaa, C. D. Johnsonb, “A comparison of two cocured damped composite torsion shafts”, *Composites Structures*, 43, pp. 115–125, 1998.

[9] R. Chandra, S. P. Singh, and K. Gupta, “Damping studies in fiber-reinforced composites- a review.”, *Composite Structures*, vol. 46, pp. 41–51, 1999.

[10] I. C. Finegan, R. F. Gibson, “Analytical modeling of damping at micromechanical level in polymer composites reinforced with coated fibers”, *Composites Science and Technology*, vol.60, pp. 3–8, 2000.

[11] R. Chandra, S. P. Singh, K. Gupta, “Micromechanical damping models for fiber-reinforced composites : a comparative study”, *Composites Part A*, vol 33, pp. 787–796, 2002.

[12] A. L. Araújo, C. M. Mota Soares, C. A. Mota Soares, and J. Herskovits, “Damping Optimization of Viscoelastic Laminated Sandwich Composite Structures”, *International Conference on Engineering Optimization*, 2008.

[13] P. Bangarubabu, K. K. Kumar, and Y. Krishna, “Damping Effect of Viscoelastic Materials on Sandwich Beams”, *International Conference on Trends in Industrial and Mechanical Engineering (ICTIME’2012)*, pp. 171–173, 2012.

[14] C. E. Beards and C. Eng, “Structural Vibration : Analysis and Damping”, *ISBN*, 1996.

[15] A. Trego and P. F. Eastman, “Optimization of Passively Damped Composite Structures”, *International Journal of Modelling and Simulation*, vol. 17, 1997.

[16] D. Jones, "*Handbook of viscoelastic vibration damping*", New York: Wiley, 2001

[17] L. F. Nielsen, "*Viscoelastic material proprieties*", 1995.

[18] J. Ciambella, M. Destrade, and R. W. Ogden, "On the ABAQUS FEA model of finite viscoelasticity", *Framework Rubber Chemistry and Technology*, vol. 82, pp. 184–193, 2009.

[19] C. Chazal, R. Pitti, "Theoretical and Numerical studies of relaxation differential approach in viscoelastic materials using generalized variables", *Journal of Theoretical and applied Mechanics*, vol.50, pp.357-375, 2012.

[20] R. Lakes, "I*n Viscoelastic Materials"*, Cambridge: Cambridge University Press, pp. 1–13, 2009.

[21] D. Roylance, "*Enginnering Vicoelasticity*", Cambridge: MIT Press, pp. 1–37, 2001.

[22] H. A. Waterman, "Relations between loss angles in isotropic linear viscoelastic materials", *Rheologica Acta*, vol. 16, pp. 31–42, 1977.

[23] A. Wineman and R. S. Lakes, "On Poisson ' s Ratio in Linearly Viscoelastic Solids", *Journal of Elasticity*, vol. 85, pp. 45–63, 2006.

[24] R. Michalczyk, "Implementation of Generalized Viscoelastic Material Model in Abaqus Code", *Logistyka*, vol. 6, 2011.

[25] A. C. Mendonça, W. S. Sousa, N. S. Soeiro, and G. V. Melo, "Caracterização de materiais viscoelásticos pelo método da viga vibrante", I Workshop de Vibração e Acústica da Região Norte, pp. 1–5, 2008.

[26] A. A. Diacenco, "*Modelagem por elementos finitos de materiais compósitos estruturais incorporando material viscoelástico para o controle passivo de vibração e ruído*", Itajubá: Federal University of Itajubá, 2010.

[27] A. Turi Edith, "*Thermal Characterization of Polymeric Materials"*, New York: Academic Press, 1997.

[28] M. Fernanda, P. Costa, C. Ribeiro, T. E. Simos, G. Psihoyios, C. Tsitouras, and Z. Anastassi, "Parameter Estimation of Viscoelastic Materials: A Test Case with Different Optimization Strategies," AIP conference Procedure, pp. 771–774, 2011.

[29] E. Barkanov, "Transient Response Analysis of Strucutres Made From Viscoelastic Materials", *International Journal for Numerical Methods in Engineering*, vol. 44, pp. 393–403, 1999.

[30] F. Mainardi and G. Sapada, "Creep , Relaxation and Viscosity Properties for Basic Fractional Models in Rheology", *The European Physical Journal*, vol. 193, pp. 133–160, 2011.

[31] M. Bulíček, J. Málek, and K. R. Rajagopal, "On Kelvin-Voigt model and its generalizations", *Evolution Equations and Control Theory*, vol. 1, pp. 17–42, 2012.

[32] Y. M. De Haan and G. M. Sluimer, "Standart linear solid model for dynamic and time dependent behaviour of bulding materials", *Heron*, vol. 46, 2001.

[33] *ABAQUS Analysis User's Manual*. Vol I, II, III, IV., 2011.

[34] M. M. Ratwani, “Composite Materials and Sandwich Structures – A Primer,” *RTO-EN-AVT*, vol. 156, pp. 1–16, 2010.

[35] S. Khan, “Bonding of sandwich structures - the facesheet/honeycomb interface - a phenomenological study”, *52nd International SAMPE Symposium and Exhibition*, 2007.

[36] S. W. Hansen, “Several related models for multilayer sandwich plates”, *Math. Models & Meth. Appl.*, vol. 14, pp. 1103–1132, 2004.

[37] G. Wang, Veeramani.Sudha, and N. M. Wereley, “Analysis of Sandwich Plates with Isotropic Face Plates and a Viscoelastic Core”, *Journal of Vibration and Acoustics*, vol. 122, 2000.

[38] J. A. Speer, “*Integrated system damping and isolation of a three dimensional structure*”, Monterey: Naval Postgraduate School, 1996.

[39] P. Dewangan, “*Passive viscoelastic constrained layer damping for structural application*”, Rourkela: National Institute of Technology Rourkela, 2009.

[40] C. T. Sun, B. V. Sankar, and V. S. Rao, “Damping and vibration control of unidirectional composite laminates using add-on viscoelastic materials”, *Journal of Sound and Vibration*, vol. 139, pp. 277–287, 1990.

[41] M. Kaufmann, “*Cost / Weight Optimization of Aircraft Structures*”, Stockolm: KTH School of Engineering Sciences, 2008.

[42] X. Huang, “Fabrication and Properties of Carbon Fibers”, *Materials*, vol. 2, no. 4, pp. 2369–2403, Dec. 2009.

[43] J. M. Silva, N. Nunes, C Z Franco, and P. . Gamboa, “Damage tolerant cork based composites for aerospace applications”, *The Aeronautical Journal*, vol. 115, 2011.

[44] O. Castro, J. M. Silva, T. Devezas, A. Silva, and L. Gil, “Cork agglomerates as an ideal core material in lightweight structures,” *Materials & Design*, vol. 31, no. 1, pp. 425–432, Jan. 2010.

[45] A. C. Composites, “Reinventing thermal protection in Aerospace applications.” .

[46] E. Balmes, “Modeling damping at the material and structure levels”, *Proceedings of IMAC-XXIV Conference & Exposition on Structural Dynamics*, 2006.

[47] J. Sun, “*Rotating Structure Modeling and Damping Measurements*”, Stockolm: Royal Institute of Technology, 2011.

[48] T. Pritz, "The Poisson's loss factor of solid viscoelastic materials", *Journal of Sound and Vibration*, 2007.

[49] J. F. Mano, “Creep-recovery behaviour of cork”, *Materials Letters*, vol. 61, no. 11–12, pp. 2473–2477, 2007.

[50] ASTM E756-98, (1998). "Standard test method for measuring vibration-damping properties of materials", ASTM, 1998.

[51] S. H. Zhang and H. L. Chen, “A study on the damping characteristics of laminated composites with integral viscoelastic layers,” *Composite Structures*, vol. 74, no. 1, pp. 63–69, 2006.

Annex A – Experimental versus Numerical results plots.

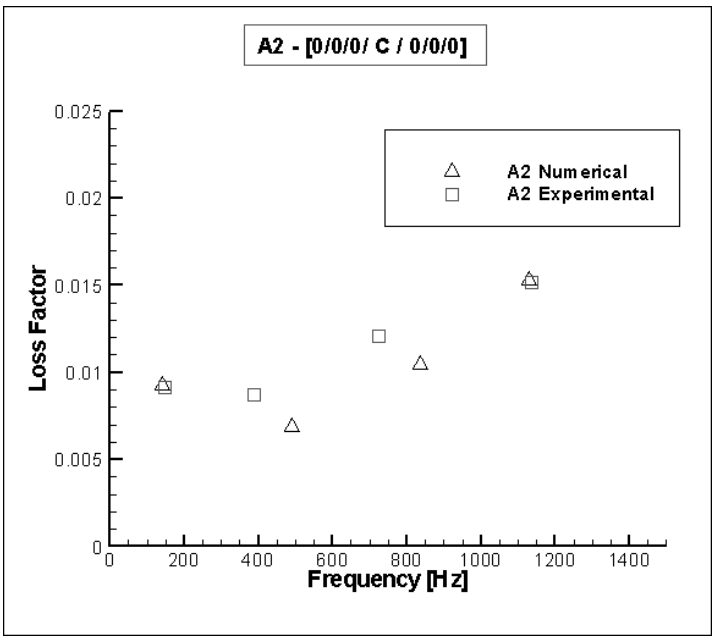

Figure A.1 – Numerical and experimental results obtained for type A2.

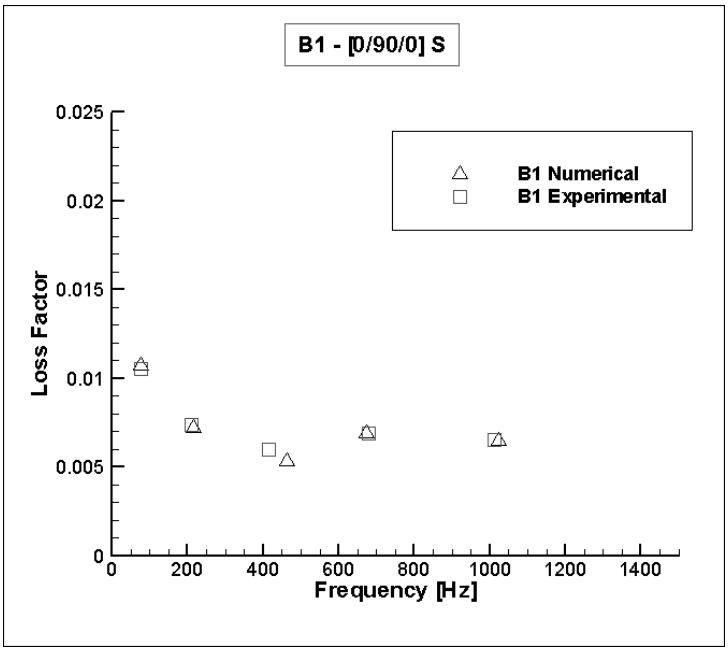

Figure A.2 – Numerical and experimental results obtained for type B1.

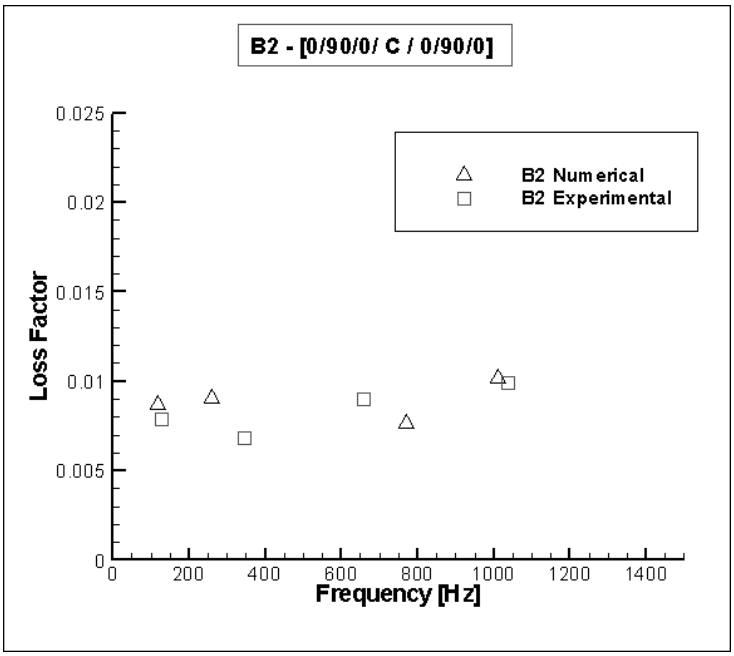

Figure A.3 – Numerical and experimental results obtained for type B2.

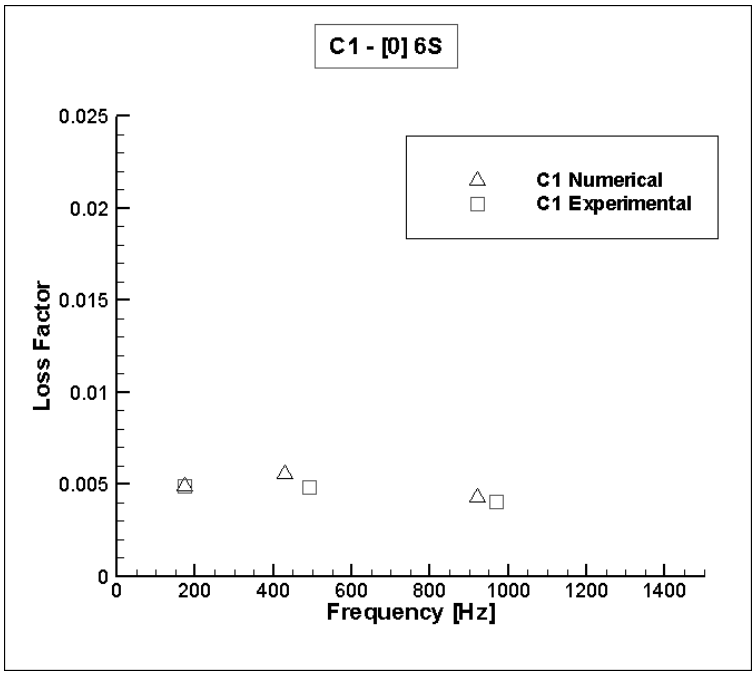

Figure A.4 – Numerical and experimental results obtained for type C1.

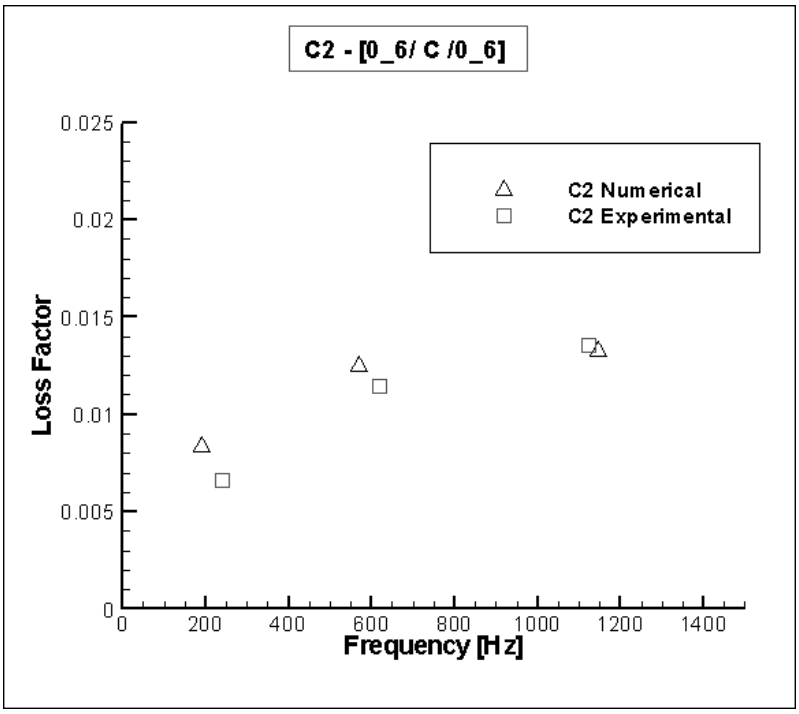

Figure A.5 – Numerical and experimental results obtained for type C2

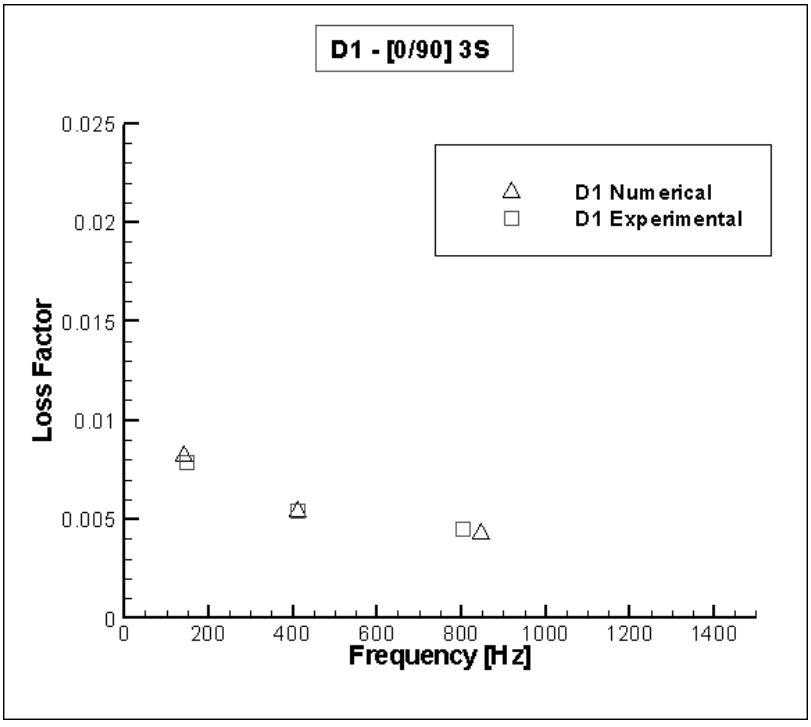

Figure A.6 – Numerical and experimental results obtained for type D1.

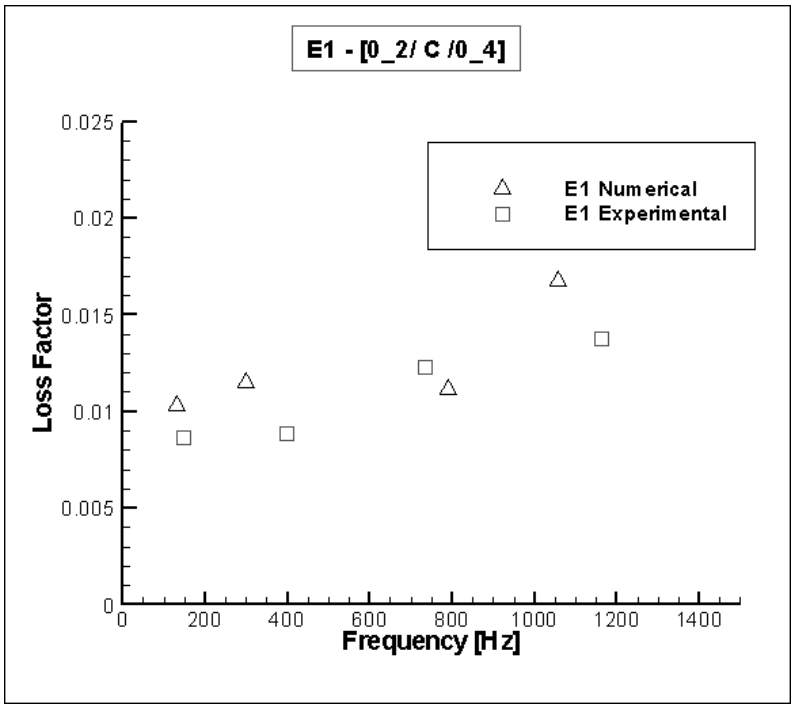

Figure A.7 – Numerical and experimental results obtained for type E1.

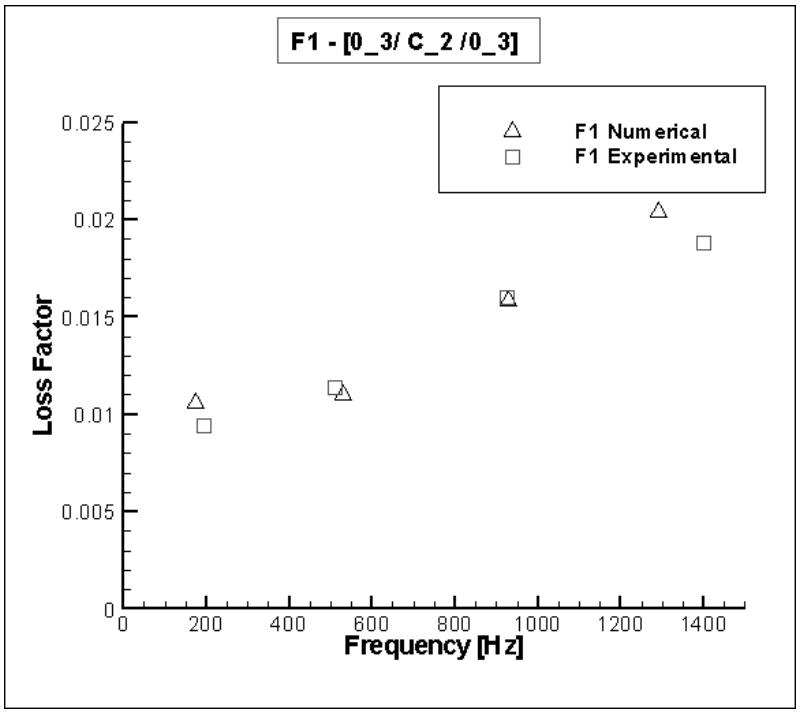

Figure A.8 – Numerical and experimental results obtained for type F1.

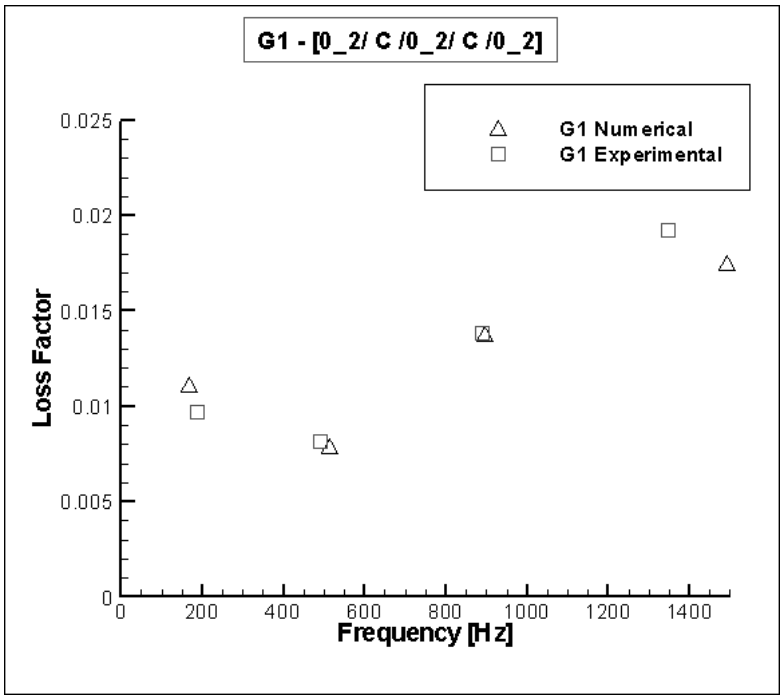

Figure A.9 – Numerical and experimental results obtained for type G1.

Annex B – Dynamic response in frequency domain plots.

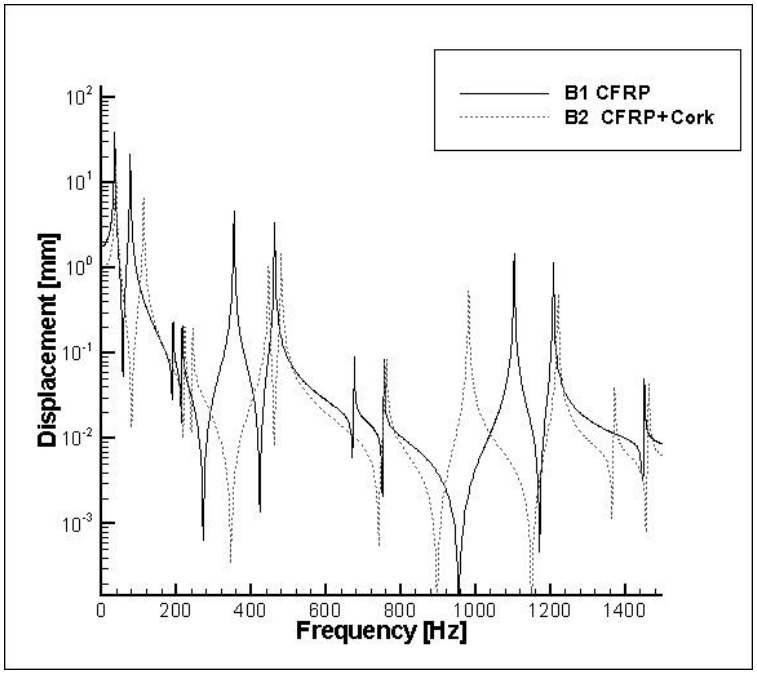

Figure B.1 – Dynamic response in frequency domain of specimens B1 and B2.

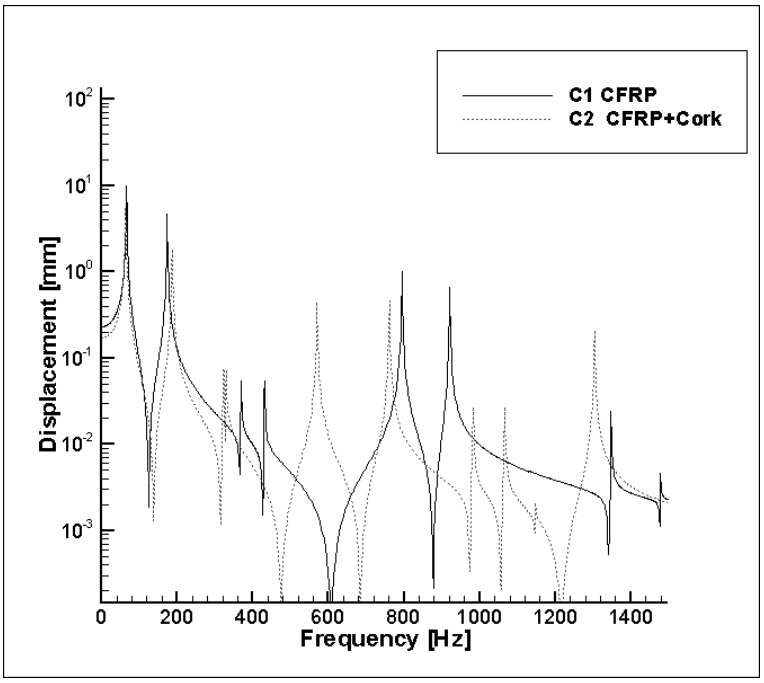

Figure B.2 – Dynamic response in frequency domain of specimens C1 and C2.

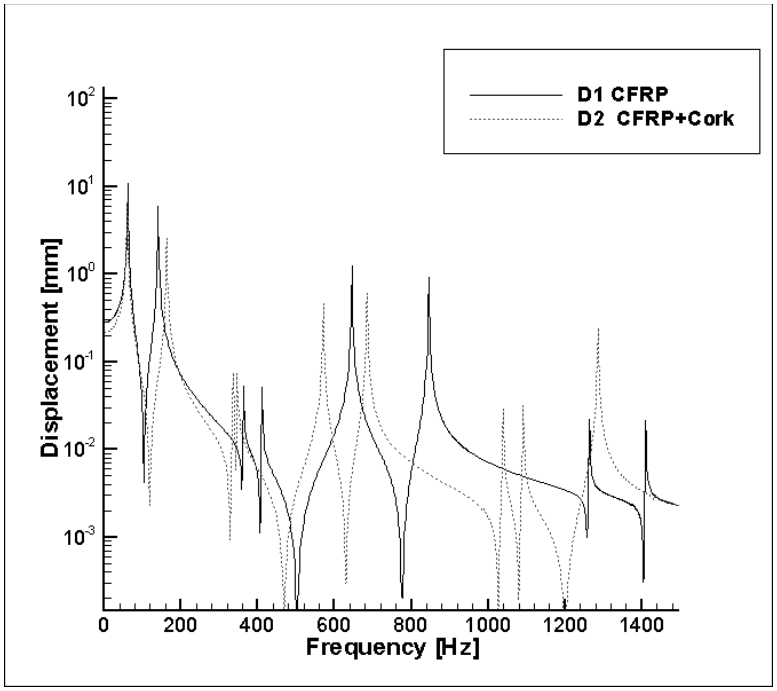

Figure B.3 – Dynamic response in frequency domain of specimens D1 and D2.

Annex C – Scientific Papers

C.1

A Passive Approach to the Development of High Performance Composite Laminates with Improved Damping Properties

J.M. Silva[1], M. Píriz[1], P.V. Gamboa[1], R. Cláudio[2,3], N. Nunes[2], and J. Lopes[1]

[1] AeroG/LAETA – Aeronautics and Astronautics Research Center, University of Beira Interior, Covilhã, Portugal
[2] Department of Mechanical Engineering, Instituto Politécnico de Setúbal, Portugal
[3] ICEMS, Instituto Superior Técnico, Universidade Técnica de Lisboa, Portugal.

Abstract

This paper explores the use of a viscoelastic material as a passive and straightforward solution towards the development of a hybrid composite material with improved damping properties. A cork based composite was elected as viscoelastic material due to its low weight combined with excellent damping properties, showing a great potential for vibration control. Two forms of specimens were considered: 1) a sandwich consisting of carbon-epoxy facesheets and a cork agglomerate core; 2) a carbon-epoxy laminate with embedded cork granulates. The experimental determination of the loss factor was based on the bandwidth method, being a determinant step to obtain relevant dynamic properties of the material for the development of an accurate computational model based on the different types of geometries.

Results are encouraging about the possible use of cork based composites as a viable passive solution to improve the damping properties of high performance composites according to the design requirements for particular applications.

Keywords: Sandwich components, viscoelastic material, composite material, structural damping, loss factor, cork.

C.2

Optimization of the Damping Properties of CFRP Laminates with Embedded Viscoelastic Layers

J.M. Silva[1], P.V. Gamboa[1], R. Cláudio[2,3], N. Nunes[2], J. Lopes[1] and M. Píriz[1]

[1] AeroG/LAETA – Aeronautics and Astronautics Research Center, University of Beira Interior, Covilhã, Portugal
[2] Department of Mechanical Engineering, Instituto Politécnico de Setúbal, Portugal
[3] ICEMS, Instituto Superior Técnico, Universidade Técnica de Lisboa, Portugal.

Abstract

This paper addresses the problem of improving the loss factor of carbon-epoxy laminates with embedded viscoelastic layers. A cork based agglomerate was elected as viscoelastic material due to its low weight combined with excellent damping properties, showing a great potential for vibration control. A micro-sandwich type geometry was adopted as this provides a good compromise between structural efficiency and easiness of inclusion of the damping material.

A numerical model was developed in order to obtain the best material configuration in terms of its damping response. Distinct design variables were considered to assess their influence in the loss factor variation, namely: damping layer thickness and its relative position within the laminate, number of viscoelastic layers and effect of different layup stacking sequences. Numerical results were compared with experimental data as this was a determinant step to obtain accurate computational models regarding the different types of geometries.

Results are encouraging about the possible use of cork based composites as a viable passive solution to improve the damping properties of high performance composites, giving rise to an increase of the loss factor as well as a change of the natural frequencies of the structure according to the design requirements for particular applications.

Keywords: Viscoelastic material, composite material, structural damping, loss factor, cork.